NASA TN D-1040

TECHNICAL NOTE

D-1040

PREDICTED PERFORMANCE OF ON-OFF SYSTEMS FOR PRECISE SATELLITE ATTITUDE CONTROL

By Stuart C. Brown

Ames Research Center
Moffett Field, Calif.

NATIONAL AERONAUTICS AND SPACE ADMINISTRATION
WASHINGTON
July 1961

NATIONAL AERONAUTICS AND SPACE ADMINISTRATION

TECHNICAL NOTE D-1040

PREDICTED PERFORMANCE OF ON-OFF SYSTEMS FOR PRECISE SATELLITE ATTITUDE CONTROL

By Stuart C. Brown

SUMMARY

An investigation has been made of the use of on-off reaction jets for precision attitude control of a satellite. Since a symmetrical vehicle is assumed, only single-axis control needs to be considered. The responses to initial disturbances and also limit-cycle characteristics for several systems have been evaluated. Calculated results indicate that realistic values of settling time and fuel consumption for the example considered can be obtained.

The performance of a given system depends on the characteristics of the error detector used. In cases where the detector output was saturated for a relatively low error input, the settling time deteriorated when a lead network was used to provide damping. This deterioration could be eliminated if a separate rate signal to produce vehicle rate limiting were available. As an alternate approach, two systems were investigated which used a timed sequence of torques and could operate with a detector output of very small linear range. Although the performance of these systems was poorer than that of the lead network system without detector saturation, the performance was better than that of the lead network system with low values of detector saturation. The effects on limit-cycle characteristics of hysteresis, lead network constants, dead zone, and thrust time delays were also investigated.

INTRODUCTION

As more sophisticated satellite payloads become feasible, more precise attitude control systems generally become necessary. An example of this trend is the orbiting astronomical observatory (ref. 1). The attitude control requirements for this project include space pointing accuracies as high as 0.1 second of arc as well as relatively high angular rate capability in order to slue from one target star to another. In addition, the target may be occulted by the earth for part of the orbit, and the vehicle must be reoriented when the target reappears.

General aspects of the attitude control problem were discussed in references 2 and 3. The use of inertia wheels for precise attitude control is discussed in reference 4. An alternate approach using on-off reaction jets, which is attractive because of its simplicity of operation, will be discussed in this report. References 5 and 6 discussed principally the limit-cycle characteristics of on-off jet control systems for cases with pointing accuracy requirements less severe than those considered here. Investigations have also been made of many of the characteristics of on-off control systems which use a linear combination of state variables to form a switching control function (ref. 7) or which use a nonlinear combination of state variables to produce a system with minimum response time to a given input or initial condition (ref. 8).

For the orbiting astronomical observatory, both a coarse and fine control mode are used because of the large dynamic range required. This report will be concerned with the characteristics of a fine control mode; that is, it will be assumed that a coarse control mode has alined the vehicle to within a set of prescribed error and error rate values. The use of microthrust jets to correct these initial errors, and the resulting low-frequency limit-cycle motion about a prescribed dead zone will be investigated. Since the vehicle is inertially balanced as closely as possible, and since the reaction jets do not introduce cross-coupling torques, coupling effects between control axes will be negligibly small. Hence the performance can be analyzed on a single degree of freedom basis. The influence of external torques due to solar, gravity, magnetic, and atmospheric effects must also be considered. These disturbances vary at rates associated with the orbital period. Since system settling times of the order of 3 minutes are desired, the external torques may be treated as constants.

An additional important effect which will be investigated is that of detector saturation. This effect may be encountered for any system for which a large dynamic range is required. While an error signal varying with amplitude over the entire control range is certainly desirable even though multiple detector ranges would be required, certain geometric and sensitivity limitations may make a continuously varying signal difficult to obtain. Two systems which use a timed torque sequence and can operate in the presence of detector saturation will be investigated.

SYMBOLS

a	magnitude of angular acceleration applied by reaction jets or average value if positive and negative values are unequal
a_1	magnitude of negative acceleration applied by reaction jets
a_2	magnitude of positive acceleration applied by reaction jets
a_e	acceleration produced by external torque
F	force applied by reaction jets
h	relay total hysteresis
l	distance from reaction jets to center of gravity
I	moment of inertia of satellite vehicle
I_{sp}	specific impulse
$K_{\dot{\theta}}$	gain of differentiating network used with linear switch-curve system
s	transform variable
t	time, sec
t_c	time required to complete one cycle for timer or rate systems
t_d	delay time approximating thrust decay
t_r	delay time approximating thrust rise
t_t	total settling time for a given initial condition
$\bar{t}_t$	average total settling time for a range of initial conditions
t_T	total settling time for an initial angular rate
T	time constant for differentiating network
W_t	fuel weight consumed during a given transient motion
W_{av}	average fuel consumption rate during limit-cycle motion
w_{av}	average normalized fuel consumption rate during limit-cycle motion, per sec

w_c normalized fuel weight required for one cycle of timer or rate systems

w_t normalized fuel weight for a given transient motion, $\frac{W_t I_{sp} l}{I}$

$\bar{w}_t$ average normalized fuel weight for a range of initial conditions

θ angular displacement

$\dot{\theta}$ angular velocity, $\frac{d\theta}{dt}$

θ_{co} maximum angular deviation during coast portion of limit cycle with no external torque

θ_d desired control accuracy of attitude angle

θ_{dz} control function dead zone of linear switch-curve system

$\dot{\theta}_d$ desired control accuracy of angular rate

θ_L saturation value of error detector

$\dot{\theta}_L$ angular-rate limit

$\dot{\theta}_{lm}$ measured value of $\dot{\theta}$ at $\theta = 0$ for rate system

$\delta\dot{\theta}$ increment in $\dot{\theta}$ produced by jet thrust during limit-cycle motion

τ torque-on time for motions near the limit-cycle condition

τ_l torque-on time for limit cycle

$\text{sgn}(\ )$ $\frac{|(\ )|}{(\ )}$

Subscript

o initial value

ANALYSIS

The characteristics of several systems which use low-thrust on-off jets for the attitude control of a satellite, such as the orbiting astronomical observatory, will be developed in this section. As stated in the introduction, only a single degree of freedom will be considered. The system will be assumed to be alined initially within a given value of error and error rate. Equations will be developed for determining settling times and fuel consumption for systems with different forms of switching logic to control the jet action. The effects of detector saturation on performance will also be included. In addition, equations for limit-cycle characteristics and the corresponding fuel consumption will also be determined. Since transient performance is of primary interest, it will be convenient to illustrate vehicle response through use of the phase plane (e.g., ref. 9).

For an application, such as the orbiting astronomical observatory, the initial errors are large in comparison with the ultimate tracking accuracy desired even if separate coarse and fine control modes are used. For instance, if an initial error of 2 minutes of arc for a fine control mode is assumed, with a desired tracking accuracy of 0.1 second of arc, the initial error would be over 1000 times the desired value. Because of the large dynamic range being considered, the analysis can be separated into two parts: (1) the settling time required for the system to recover from an initial error to within a desired value, and (2) the transition into a limit-cycle motion. For the astronomical observatory program, every effort is made to reduce the magnitude of the external torques because of the high pointing accuracy required. Initial estimates were that by careful balance of inertial, magnetic, solar reflecting, and aerodynamic properties, average torques could be reduced to the order of 100 dyne-cm for a vehicle with moments of inertia of about 10^{10}gm cm^2 (ref. 1). Although this value of torque is small in comparison with later estimates due to subsequent changes in the vehicle, it will be adequate for use in the example calculations which will be shown in this report. Since the applied torque to be considered will be about 100 times larger than the external torque, the latter will affect only the limit-cycle motion. Similarly, other properties such as dead zones and time delays significantly influence only the limit-cycle characteristics. However, it should be noted that calculations of time to settle to within a given error could be affected if this error were sufficiently close to errors encountered during limit-cycle motion.

Since external spring and damping torques acting on the controlled vehicle can be neglected, the resulting vehicle motion which results from the control system applied torques can be given approximately in analytical form. An analog computer was used mainly as a check on the calculated results from the equations which will be developed.

Recovery From Initial Errors

Common characteristics of the systems to be considered will be discussed first. A block diagram is shown in figure 1. The angular error is measured by an error detector with assumed perfect dynamic characteristics. The switching function, for which several types will be compared, determines the direction of the torque to be applied to the vehicle. The function actuates the appropriate relay which controls an on-off type valve that applies a torque in the proper direction. The resulting equation of motion is linear during the interval the applied torque is constant. When the applied torque switches sign, continuity in θ and $\dot{\theta}$ is maintained so that initial conditions for the suceeding motion are the same as the end conditions for the previous motion. Since the vehicle damping and spring forces can be neglected, and since the applied torque is much greater than the assumed disturbance torques, the applied torque Fl, produces a constant acceleration

$$\ddot{\theta} = \pm a = \frac{Fl}{I} \tag{1}$$

The resulting vehicle motions become

$$\dot{\theta} = \dot{\theta}_o \pm at \tag{2}$$

$$\theta = \theta_o + \dot{\theta}_o t \pm (1/2)at^2 \tag{3}$$

The zero subscripts refer to conditions existing when the torque is initially applied.

If no torque is applied, the vehicle coasts at a constant angular rate

$$\dot{\theta} = \dot{\theta}_o \tag{4}$$

$$\theta = \theta_o + \dot{\theta}_o t \tag{5}$$

The zero subscripts for this case refer to initial conditions at the beginning of the coast period.

The switching times are determined by functions of the state of the system which will be described by the variables θ and $\dot{\theta}$. A convenient way of representing these motions is through use of the phase plane

(ref. 9). When time is eliminated between equations (2) and (3), the motions in the phase plane become (1) for the constant torque case

$$\theta = \theta_o - \frac{\dot{\theta}_o^2}{\pm 2a} + \frac{\dot{\theta}^2}{\pm 2a} \tag{6}$$

and (2) for the coast case

$$\dot{\theta} = \dot{\theta}_o$$

Complete motion histories can be obtained by piecing together these trajectory segments.

To provide a quantitative comparison of different systems, two parameters are of interest: (1) settling time, that is, the time required for the system to recover and remain within a certain desired amplitude and (2) the fuel consumption during this motion. The total settling time required, t_t, for a given motion is determined from a series of trajectory segments as

$$t_t = \sum_{j=1}^{J} \left| \frac{\Delta \dot{\theta}}{a} \right| + \sum_{k=1}^{K} \left| \frac{\Delta \theta}{\dot{\theta}} \right| \tag{7}$$

where J is the number of torque-on trajectory segments, K is the number of torque-off trajectory segments, and $\Delta(\ )$ denotes the change in a variable over a trajectory segment. The weight of the fuel consumed during the motion can be obtained (assuming a constant specific impulse for all operating conditions) by the sum of the changes in angular rate of the torque-on trajectory segments.

$$W_t = \frac{I w_t}{I_{sp} l} \tag{8}$$

where

$$w_t = \sum_{j=1}^{J} |\Delta \dot{\theta}|$$

Settling time and fuel consumption for several systems will be compared. Since a nonlinear system may be tuned to a particular set of initial conditions, a range of sets of initial conditions, each sufficient to define the initial state of the system, must be investigated.

For this report initial values of angle and angular rate errors will be used.[1] For each system, an average value of settling time and fuel consumption will be determined, based on the range of initial conditions to be considered. The selected conditions should be as realistic as possible to provide a valid comparison between the systems. A simplified set of initial conditions, which are distributed along a line and normalized to a desired angular tracking accuracy θ_d, that was used for this report is shown in sketch (a).

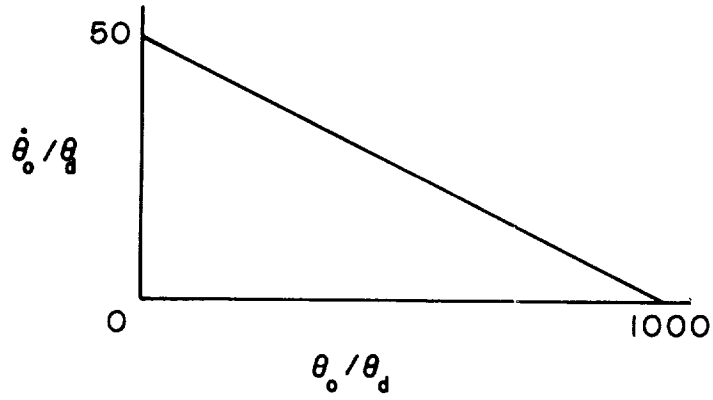

Sketch (a)

This distribution is representative of that which could be introduced by a coarse-control on-off system for which the switch curve is linear. In addition, the probability of occurrence of all combinations of θ_o/θ_d and $\dot{\theta}_o/\theta_d$ was assumed to be equal. After a direction of integration, dx, is defined along the line of initial conditions, and the probability of occurrence of the initial conditions is set equal to unity so that the length of the line in the direction x is unity, the previous equation reduces to

$$\bar{t}_t = \int_o^1 t_t \left(\frac{\theta_o}{\theta_d}, \frac{\dot{\theta}_o}{\theta_d}\right) dx \qquad (9)$$

---

[1] If a joint probability distribution of initial values of angle and angular rate is known, $p(\theta_o, \dot{\theta}_o)$, then an average value of settling time can be determined by the following integration over a surface, S, in the $\theta_o, \dot{\theta}_o$ plane,

$$\bar{t}_t = \int_S \int p(\theta_o, \dot{\theta}_o) t(\theta_o, \dot{\theta}_o) d\theta_o d\dot{\theta}_o$$

The average settling times can then be compared for several systems.

The integration was performed numerically along the line describing the initial conditions shown in sketch (a). The average values of settling time, $\bar{t}_t$, were obtained by evaluating equation (9) by use of Simpson's rule from calculated values of t_t at equally spaced increments of θ_o/θ_d and $\dot{\theta}_o/\theta_d$. The average values of normalized fuel weight, $\bar{w}_t/\theta_d$, were calculated by a similar numerical integration.

The equations used to determine system settling time and fuel consumption during recovery from an initial error will be developed next.

Linear switch curve system.- For this system, the switching logic used is of the following form:

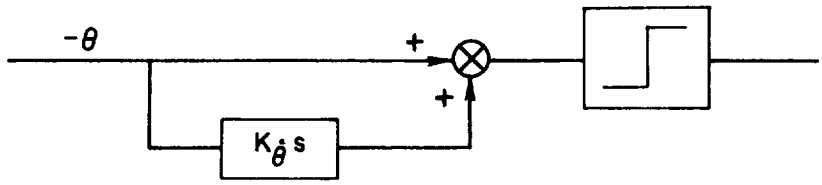

Sketch (b)

The rate signal is assumed to be formed by a perfect lead network. The effect of the time constant of the network was found to be important only during limit-cycle motion and, hence, was neglected. The resulting motion is then determined by the equation

$$\ddot{\theta} = -a \operatorname{sgn}(\theta + K_{\dot{\theta}}\dot{\theta})$$

Thus, the torque changes sign whenever the quantity $\theta + K_{\dot{\theta}}\dot{\theta}$ changes sign. For convenience, a unit gain is associated with θ.

To obtain the total settling time, the motions shown in sketch (c) are separated into three parts:

(1) The time required to first reach the switch curve from a given set of initial conditions,

(2) The time required during which the trajectory overshoots the switch curve when it is intersected, and

(3) The time during which the motion subsides as commanded by the switch curve until the desired attitude angle is reached.

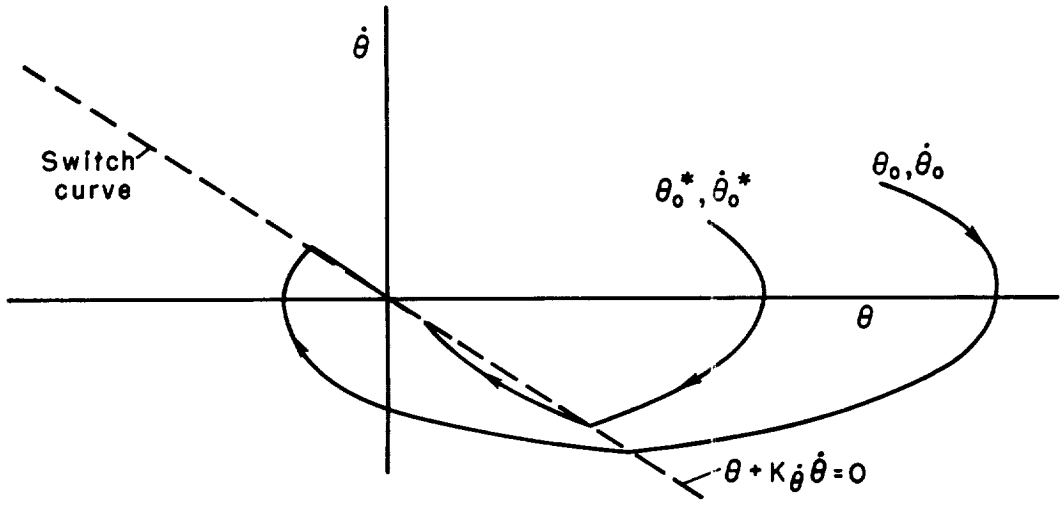

Sketch (c)

Equations for total settling time and fuel consumption may be obtained from equations for the trajectory segments, the switch-curve equation, and relations describing the time required and fuel consumption for each trajectory segment. A derivation of the equations is given in the appendix. The equations to be given in this report for settling times and fuel consumption will be valid for a range of initial conditions at least within the first quadrant of the phase plane. This is sufficient to evaluate the initial conditions shown in sketch (a). While equations could be written for more general initial conditions, they tend to become rather cumbersome.

The time, t_1, required to reach the switch curve from initial conditions θ_o, $\dot{\theta}_o$ is

$$t_1 = \frac{\dot{\theta}_o}{a} - K_{\dot{\theta}} + \sqrt{K_{\dot{\theta}}^2 + \left(\frac{\dot{\theta}_o}{a}\right)^2 + \frac{2\theta_o}{a}} \tag{10}$$

$$\dot{\theta}_1 = \dot{\theta}_o - at_1 \tag{11}$$

The total time required to settle to a given amplitude θ_d can be determined by the following equation

$$t_t = t_1 + (6K_{\dot{\theta}} - \frac{2\dot{\theta}_1}{a})(N - 1) - 4K_{\dot{\theta}} \sum_{n=2}^{N} n$$

$$+ K_{\dot{\theta}} \log_e \left| \frac{1}{\theta_d} \left[- K_{\dot{\theta}}\dot{\theta}_1 - 2aK_{\dot{\theta}}^2(N - 1) \right] \right| \tag{12}$$

where N is the nearest integral value of $\frac{-\dot{\theta}_1}{2aK_{\dot{\theta}}} + 1$ and $\log_e |\quad| = 0$ if $|\quad| < 1$. The quantity N represents the total number of trajectory segments which terminate on the switch curve prior to the motion which subsides along the switch curve. The last term in equation (12) represents the time during which motion is along the switch curve and is the time to damp for a first-order linear system with a root equal to $-1/K_{\dot{\theta}}$.

The fuel consumption is calculated from the summation of momentum or angular rate changes (eq. (8))

A 498

$$w_t = \dot{\theta}_o + 2N' \left(2aK_{\dot{\theta}} - \dot{\theta}_1\right) - 4aK_{\dot{\theta}} \sum_{n=1}^{N'} n \qquad (13)$$

where N′ is the nearest integral value of

$$\frac{-\dot{\theta}_1}{2aK_{\dot{\theta}}} + 0.5$$

The quantity N′ represents the total number of trajectory segments with the angular note at the end of the segment of opposite sign from that at the beginning of the segment. For the remaining portion of the motion which is represented by a linear system, a sufficiently wide dead zone along the switch curve is assumed so that the fuel consumed is only that required to reduce the angular rate to zero.

Minimum settling time system with nonlinear switch curve.- This system brings the vehicle to rest in a minimum time for an arbitrary set of initial conditions (ref. 8) as shown in sketch (d).

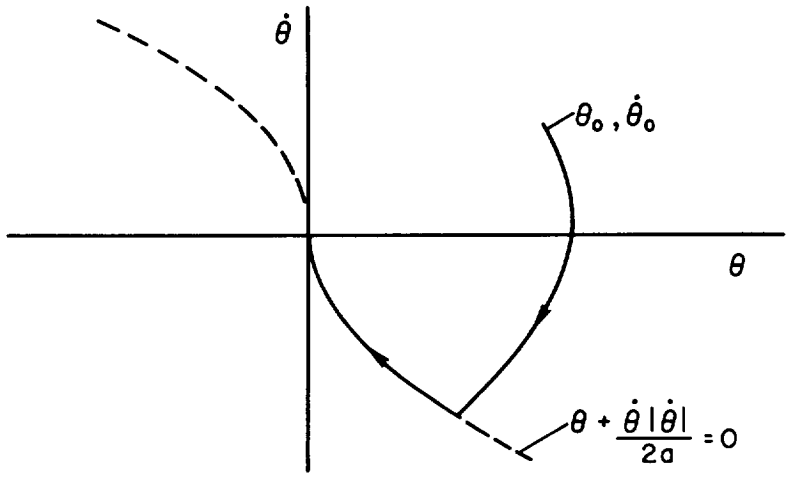

Sketch (d)

The resulting motion obtained through use of this switch curve is given by the equation

$$\ddot{\theta} = -a \operatorname{sgn}\left(\theta + \frac{\dot{\theta}|\dot{\theta}|}{2a}\right)$$

The total settling time equation becomes

$$t_t = \frac{\dot{\theta}_o}{a} + 2\sqrt{\frac{\theta_o}{a} + \frac{\dot{\theta}_o^2}{2a^2}} \tag{14}$$

The fuel consumption is simply

$$w_t = at_t = \dot{\theta}_o + 2\sqrt{a\theta_o + \frac{\dot{\theta}_o^2}{2}} \tag{15}$$

Note that these equations represent the time and fuel required to bring the vehicle to zero error and error rate rather than to a given small error, as was the case for the previous system. However, the time and fuel difference is negligible for this system because of the large error range to be considered.

Rate-limited system.- This system limits the maximum rate as shown in sketch (e).

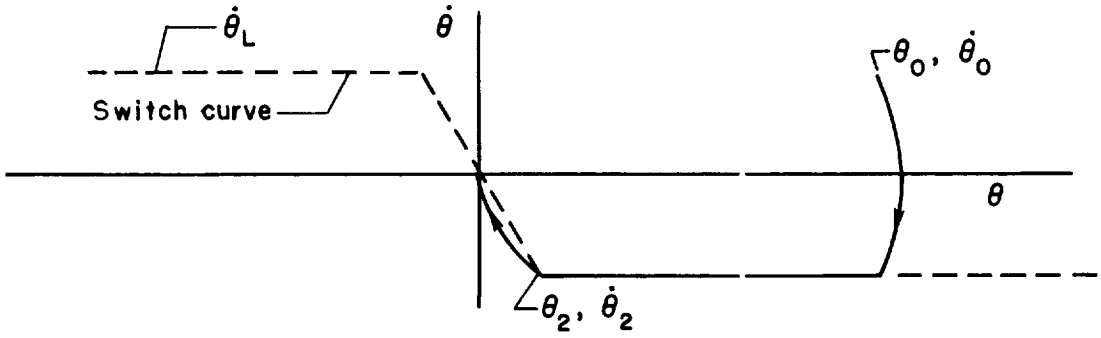

Sketch (e)

The intersection at $\theta_2,\dot{\theta}_2$ was selected so that no overshoot occurred at the origin. A sufficiently wide dead zone was assumed so that coasting would occur during rate limiting. The equation for total settling time is

$$t_t = \frac{\dot{\theta}_o}{a} + \frac{\dot{\theta}_L}{a} + \frac{\theta_o}{\dot{\theta}_L} + \frac{\dot{\theta}_o^2}{2a\dot{\theta}_L} \tag{16}$$

The equation for fuel consumption is

$$w_t = \dot{\theta}_o + 2\dot{\theta}_L \tag{17}$$

The rate limited system can be adjusted to yield a lower fuel consumption for a given settling time than other systems since fuel consumption is proportional to changes in $\dot{\theta}$. This minimum is obtained by adjusting the rate limit to the minimum value possible to still achieve the desired settling time for the system.

System with detector saturation.- The form of detector saturation being considered is shown in sketch (f).

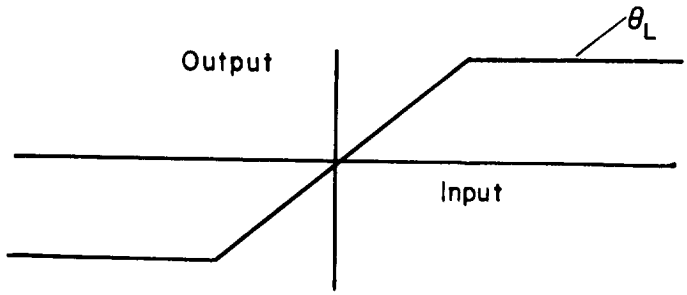

Sketch (f)

Since the rate signal is assumed to be determined by differentiation of the detector signal, then the rate signal is unobtainable during detector saturation. These combined effects may cause a considerable amount of overshoot, as shown in sketch (g), and result in a deterioration of settling time and fuel consumption.

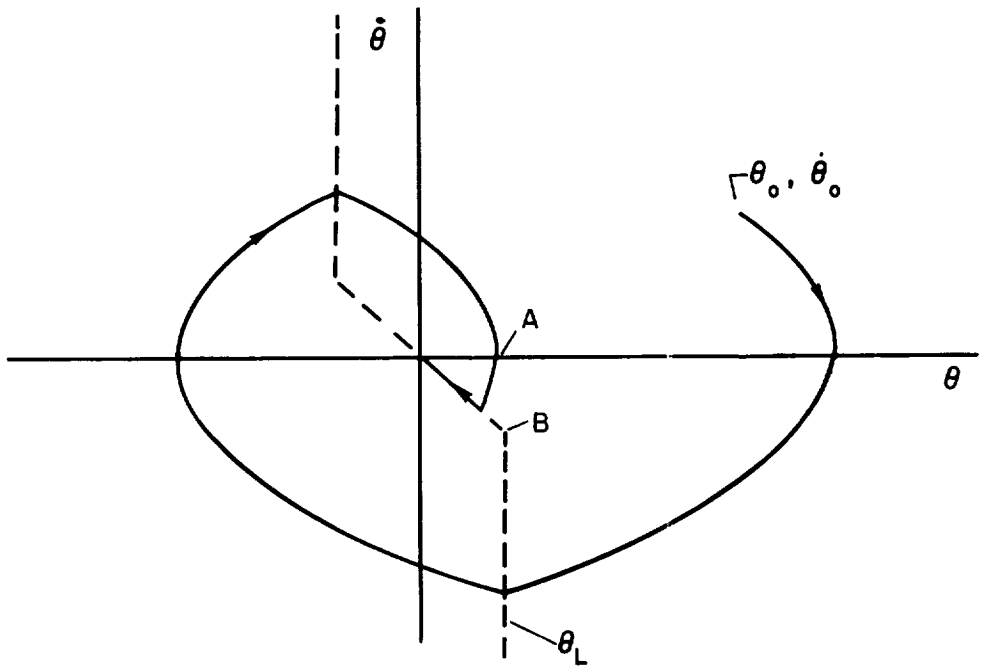

Sketch (g)

Point A is the last point the trajectory intersects on the θ axis before the portion of the switch curve below the θ_L limit is intersected. Point B is the intersection of the saturated part of the switch curve with a selected switch curve for errors less than the detector saturation value. The time required to reach point A is

$$t_A = \frac{\dot{\theta}_o}{a} + 2\sqrt{2/a} \sum_{m=1}^{M} \sqrt{\theta_o + \frac{\dot{\theta}_o^2}{2a} + (1 - 2m)\theta_L} \qquad (18)$$

where M is the nearest integral value of $\frac{\theta_o}{2\theta_I} + \frac{\dot{\theta}_o^2}{4a\theta_L} - \frac{\dot{\theta}_B^2}{4a\theta_L}$. Geometrically, M + 1 represents the number of intersections of the trajectory with the θ axis. If a linear switch curve is used below saturation values, the total settling time is obtained by adding the times calculated from equations (18) and (12). The time from equation (14) is used in place of equation (12) if a minimum time switch curve is used. The initial values to be used with either of the latter equations are the coordinates of point A.

$$|\theta_A| = \theta_o + \frac{\dot{\theta}_o^2}{2a} - 2M\theta_L$$

$$\dot{\theta}_A = 0$$

The fuel required to reach point A is

$$w_A = at_A = \dot{\theta}_o + 2\sqrt{2a} \sum_{m=1}^{M} \sqrt{\theta_o + \frac{\dot{\theta}_o^2}{2a} + (1 - 2m)\theta_L} \qquad (19)$$

The total fuel expended to decrease to a given amplitude is obtained by the sum of equations (13) and (19) for the linear switch-curve case, or the sum of equations (15) and (19) for the minimum time switch curve.

Timer system.- For cases in which detector saturation effects become important, a system which uses a timer to control torques can be desirable. Since changes in angular rates are proportional to time for a vehicle with only inertial moments, knowledge of the state of the vehicle can be obtained from a time and amplitude measurement. A timer can then be used to program switching times to bring the system to rest.

The motion for a system which would require only the direction of error beyond a given dead zone for the detector signal is shown by sketch (h).

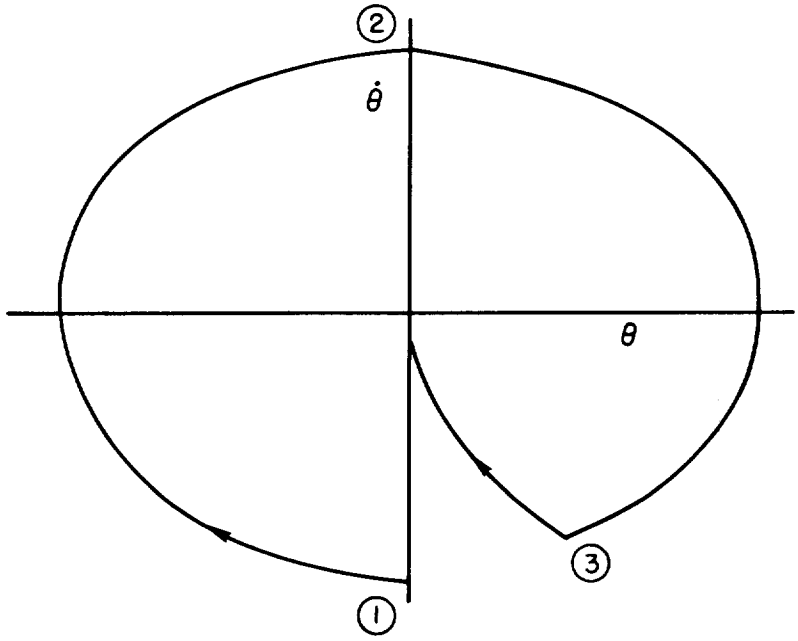

Sketch (h)

At point 1, a constant positive torque is applied. After a period of time, $t_2 = 2|\dot{\theta}_1|/a$, point 2 is reached. At point 2 the torque is switched to a negative value and is applied for $(1/2 + \sqrt{2}/4)t_2$. At point 3, positive torque is applied for $(\sqrt{2}/4)t_2$, and the system is then at zero displacement and rate. For perfect time measurement and exactly equal positive and negative torques, the final switch point, 3, is the same as a point on the previous minimum settling time curve. The total settling time is

$$t_t = (3 + \sqrt{2}) \frac{|\dot{\theta}_1|}{a} \tag{20}$$

Fuel consumption is given by the equation

$$w_t = at_t = (3 + \sqrt{2})|\dot{\theta}_1 \tag{21}$$

Since the system operates with an open loop for large portions of the trajectory, the effects of unequal magnitudes of the positive and negative applied accelerations, a_1 and a_2, should be investigated. The resulting equations will also apply for cases with equal applied torques but with a constant disturbing torque. The equations used for calculating settling time and fuel consumption will depend upon the relative magnitudes of the two accelerations.

Motions of the system for one cycle with unsymmetrical accelerations are shown in sketch (i).

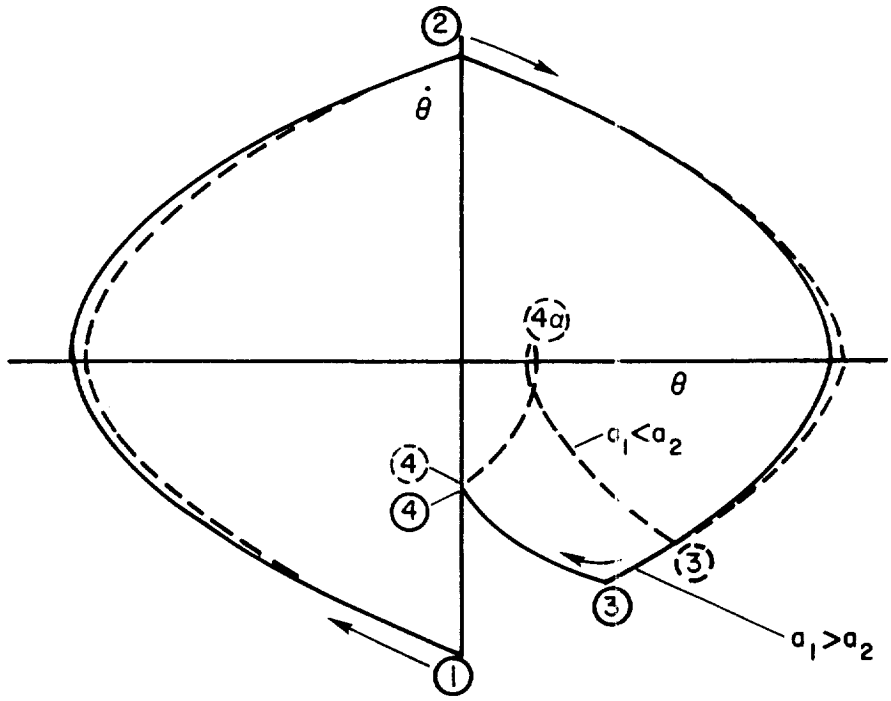

Sketch (i)

Note that the relative magnitudes of the applied accelerations cause the system to either overshoot (solid curve) or undershoot (dotted curve) the zero angle at the conclusion of the timed torque sequence. If undershoot occurs (point 4α), that is, if the system does not return to zero angle in the given time, negative acceleration is immediately applied until zero angle is reached. For either case, the cycle is then repeated until the residual angular rate at zero amplitude is within a desired value. In the subsequent equations to be given for this system, a small dead zone is assumed which represents the desired tracking accuracy, θ_d. Since this value is very small in comparison with the initial motions, it is not shown in the sketches.

Case I, overshoot ($a_1 > a_2$): For this case, the system will reach zero amplitude before the angular rate is zero. First consider only an initial angular rate $\dot{\theta}_1$. The settling time for the first cycle can be expressed in dimensionless form as

$$\frac{at_c}{|\dot{\theta}_1|} = \frac{at_2}{|\dot{\theta}_1|} + \frac{at_3}{|\dot{\theta}_1|} + \frac{at_4}{|\dot{\theta}_1|} \tag{22}$$

where

$$\frac{at_2}{|\dot{\theta}_1|} = 2\left(\frac{a}{a_2}\right)$$

$$\frac{at_3}{|\dot{\theta}_1|} = \left(1 + \frac{\sqrt{2}}{2}\right)\left(\frac{a}{a_2}\right)$$

$$\frac{at_4}{|\dot{\theta}_1|} = \left|\frac{\dot{\theta}_3}{\dot{\theta}_1}\right| \frac{a}{a_2} - \sqrt{\left(\frac{\dot{\theta}_3}{\dot{\theta}_1}\frac{a}{a_2}\right)^2 - \frac{2(\theta_3 - \theta_d)\,a^2}{a_2\,\dot{\theta}_1^2}}$$

$$\left|\frac{\dot{\theta}_3}{\dot{\theta}_1}\right| = -1 + \left(\frac{a_1}{a}\right)\frac{at_3}{|\dot{\theta}_1|}$$

$$\frac{a(\theta_3 - \theta_d)}{\dot{\theta}_1^2} = \frac{at_3}{|\dot{\theta}_1|} - \frac{1}{2}\frac{a_1}{a}\left(\frac{at_3}{\dot{\theta}_1}\right)^2$$

The ratio of initial to final rates is

$$\left|\frac{\dot{\theta}_4}{\dot{\theta}_1}\right| = \left|\frac{\dot{\theta}_3}{\dot{\theta}_1}\right| - \left(\frac{a_2}{a}\right)\frac{at_4}{|\dot{\theta}_1|} \tag{23}$$

The fuel consumption for the cycle is

$$w_c = 3|\dot{\theta}_1| + 2|\dot{\theta}_3| - |\dot{\theta}_4|$$

The total settling time can be expressed as a geometric series of the settling times for each cycle so that the total torque-on time required to subside to a desired angular rate, $\dot{\theta}_d$, is

$$\frac{at_T}{|\dot{\theta}_1|} = \frac{at_c}{|\dot{\theta}_1|}\left(\frac{1 - |\dot{\theta}_d/\dot{\theta}_1|}{1 - |\dot{\theta}_4/\dot{\theta}_1|}\right) \tag{24}$$

Note that the ratio $\dot{\theta}_d/\dot{\theta}_1$ does not represent, in general, a ratio that can be obtained from an integral number of cycles. However, if $\dot{\theta}_d$ is small in comparison with $\dot{\theta}_1$, the effect of the discrepancy in the final value of $\dot{\theta}$ on total time is negligible. The time required to cross the dead zone becomes significant as the angular rate becomes small. If $\dot{\theta}_d$ and θ_d are small in comparison with the maximum values of $\dot{\theta}$ and θ obtained during the first cycle, then the effect of dead zone on settling time can be approximately expressed by the equation

$$t_z = \frac{4\theta_d}{\dot{\theta}_d}\left(\frac{1 - |\dot{\theta}_d/\dot{\theta}_1|}{1 - |\dot{\theta}_4/\dot{\theta}_1|}\right) \tag{25}$$

For arbitrary initial conditions, the total settling time becomes

$$t_t = t_1 + t_T + t_z$$

or

$$t_t = t_1 + \left(t_c + \frac{4\theta_d}{\dot{\theta}_d}\right)\left(\frac{1 - |\dot{\theta}_d/\dot{\theta}_1|}{1 - |\dot{\theta}_4/\dot{\theta}_1|}\right) \tag{26}$$

where

$$t_1 = \frac{\dot{\theta}_o}{a_1} + \sqrt{\left(\frac{\dot{\theta}_o}{a_1}\right)^2 + \frac{2\theta_o}{a_1}}$$

$$\dot{\theta}_1 = \dot{\theta}_o - a_1 t_1$$

The fuel consumption is

$$w_t = \dot{\theta}_o + |\dot{\theta}_1| + w_c\left(\frac{1 - |\dot{\theta}_d/\dot{\theta}_1|}{1 - |\dot{\theta}_4/\dot{\theta}_1|}\right) \tag{27}$$

Case II, undershoot ($a_1 < a_2$): The first cycle is shown in the previous sketch. When undershoot results at the end of the last timed interval (point 4α), opposite torque is applied immediately till zero amplitude is reached. The time for the first cycle is expressed as

$$\frac{at_c}{|\dot{\theta}_1|} = \frac{at_2}{|\dot{\theta}_1|} + \frac{at_3}{|\dot{\theta}_1|} + \frac{at_{4\alpha}}{|\dot{\theta}_1|} + \frac{at_4}{|\dot{\theta}_1|} \tag{28}$$

where

$$\frac{at_{4\alpha}}{|\dot{\theta}_1|} = \frac{a\sqrt{2}}{2a_2}$$

$$\frac{at_4}{|\dot{\theta}_1|} = \frac{\dot{\theta}_{4\alpha}}{|\dot{\theta}_1|}\frac{a}{a_1} + \sqrt{\left(\frac{\dot{\theta}_{4\alpha}}{\dot{\theta}_1}\frac{a}{a_1}\right)^2 + \frac{2(\dot{\theta}_{4\alpha} - \dot{\theta}_d)a^2}{a_1\dot{\theta}_1^2}}$$

$$\frac{\dot{\theta}_{4\alpha}}{|\dot{\theta}_1|} = \left(1 + \frac{\sqrt{2}}{2}\right)\left(1 - \frac{a_1}{a_2}\right)$$

$$\frac{a(\theta_{4\alpha} - \theta_d)}{\dot{\theta}_1^2} = \frac{a(\theta_3 - \theta_d)}{\dot{\theta}_1^2} - \left|\frac{\dot{\theta}_3}{\dot{\theta}_1}\right|\frac{at_{4\alpha}}{|\dot{\theta}_1|} + \frac{1}{2}\frac{a_2}{a}\left(\frac{at_{4\alpha}}{\dot{\theta}_1}\right)^2$$

The equations for the remaining quantities in equation (28) are the same as those for Case I.

The ratio of final to initial rates is

$$\left|\frac{\dot{\theta}_4}{\dot{\theta}_1}\right| = -\frac{\dot{\theta}_{4\alpha}}{|\dot{\theta}_1|} + \frac{a_1}{a}\frac{at_4}{|\dot{\theta}_1|} \tag{29}$$

To find total settling time, equations (29) and (28) are substituted into equation (26). The total fuel consumption is obtained by equation (27) with

$$w_c = 3|\dot{\theta}_1| + 2|\dot{\theta}_3| + 2|\dot{\theta}_{4\alpha}| + |\dot{\theta}_4| \tag{30}$$

Modified timer system.- As will be shown in the discussion, the performance of the timer system deteriorates considerably if the applied torques are very unequal. One method for improving this limitation is to initiate the corrective torque sequence only when the error returns to the same sign that was present while the time measurement was made. This system is illustrated in sketch (j).

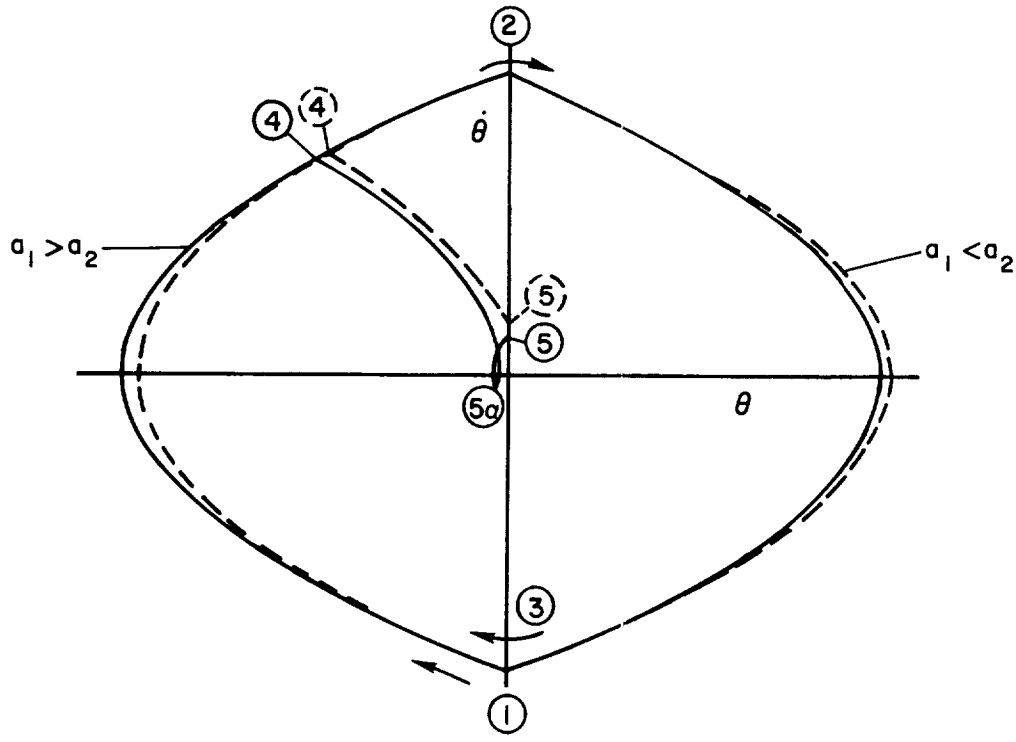

Sketch (j)

The operation of the system is as follows. The time to travel from point 1 to point 2 (t_2) is measured with a constant positive torque applied. A negative torque is then applied to drive the system to point 3. At point 3, a positive torque is applied for $(1/2 + \sqrt{2}/4)t_2$. At point 4, a positive torque is applied for $(\sqrt{2}/4)t_2$. Again, differences in magnitude of positive or negative torques will cause the system to undershoot or overshoot the origin.

Case I, undershoot ($a_1 > a_2$): For an initial angular rate $\dot{\theta}_1$, the settling time for the first cycle can be expressed as

$$\frac{at_c}{|\dot{\theta}_1|} = \frac{at_2}{|\dot{\theta}_1|} + \frac{at_3}{|\dot{\theta}_1|} + \frac{at_4}{|\dot{\theta}_1|} + \frac{at_{5\alpha}}{|\dot{\theta}_1|} + \frac{at_5}{|\dot{\theta}_1|} \tag{31}$$

where

$$\frac{at_2}{|\dot{\theta}_1|} = 2\left(\frac{a}{a_2}\right)$$

$$\frac{at_3}{|\dot{\theta}_1|} = 2\left(\frac{a}{a_1}\right)$$

$$\frac{at_4}{|\dot{\theta}_1|} = \left(1 + \frac{\sqrt{2}}{2}\right)\frac{a}{a_2}$$

$$\frac{at_{5\alpha}}{|\dot{\theta}_1|} = \frac{\sqrt{2}}{2}\,\frac{a}{a_2}$$

$$\frac{at_5}{|\dot{\theta}_1|} = -\frac{\dot{\theta}_{5\alpha}a}{|\dot{\theta}_1|\,a_2} + \sqrt{\left(\frac{\dot{\theta}_{5\alpha}}{|\dot{\theta}_1|}\,\frac{a}{a_2}\right)^2 - \frac{2(\theta_{5\alpha} + \theta_d)a^2}{a_2\dot{\theta}_1{}^2}}$$

$$\frac{\dot{\theta}_{5\alpha}}{|\dot{\theta}_1|} = \frac{\sqrt{2}}{2}\left(1 - \frac{a_1}{a_2}\right)$$

$$\frac{a(\theta_4 + \theta_d)}{\dot{\theta}_1{}^2} = -\frac{1}{4}\,\frac{a}{a_2}$$

$$\frac{a(\theta_{5\alpha} + \theta_d)}{\dot{\theta}_1{}^2} = \frac{1}{4}\,\frac{a}{a_2}\left(1 - \frac{a_1}{a_2}\right)$$

The ratio of final to initial rates for the cycle is

$$\left|\frac{\dot{\theta}_5}{\dot{\theta}_1}\right| = \frac{\dot{\theta}_5\alpha}{|\dot{\theta}_1|} + \frac{a_2}{a}\frac{at_5}{|\dot{\theta}_1|} \tag{32}$$

Case II, overshoot ($a_1 < a_2$):

$$\frac{at_c}{|\dot{\theta}_1|} = \frac{at_2}{|\dot{\theta}_1|} + \frac{at_3}{|\dot{\theta}_1|} + \frac{at_4}{|\dot{\theta}_1|} + \frac{at_5}{|\dot{\theta}_1|} \tag{33}$$

where

$$\frac{at_5}{|\dot{\theta}_1|} = \frac{a}{a_1}\frac{\sqrt{2}}{2} - \sqrt{\frac{1}{2}\left(\frac{a}{a_1}\right)^2 + \frac{2(\theta_4 + \theta_d)a^2}{\dot{\theta}_1^2 a_1}}$$

The ratio of final to initial rates is

$$\left|\frac{\dot{\theta}_5}{\dot{\theta}_1}\right| = \frac{\sqrt{2}}{2} - \frac{a_1}{a}\frac{at_5}{|\dot{\theta}_1|} \tag{34}$$

The equations for the remaining quantities in equation (33) are the same as those for Case I. Total settling time and fuel consumption can be found in a manner similar to that used for the previous timer system.

Rate system.- Another system that requires only a small error range for the detector is one that uses a lead network so that angular rate and angle can both be determined while the error is within the detector range. While a greater error range is required for this case than for the previous one in order to determine the rate, it still can be quite small. After the angular rate at zero error is determined, a timed torque sequence is initiated to bring the system to rest. A typical trajectory is shown in sketch (k).

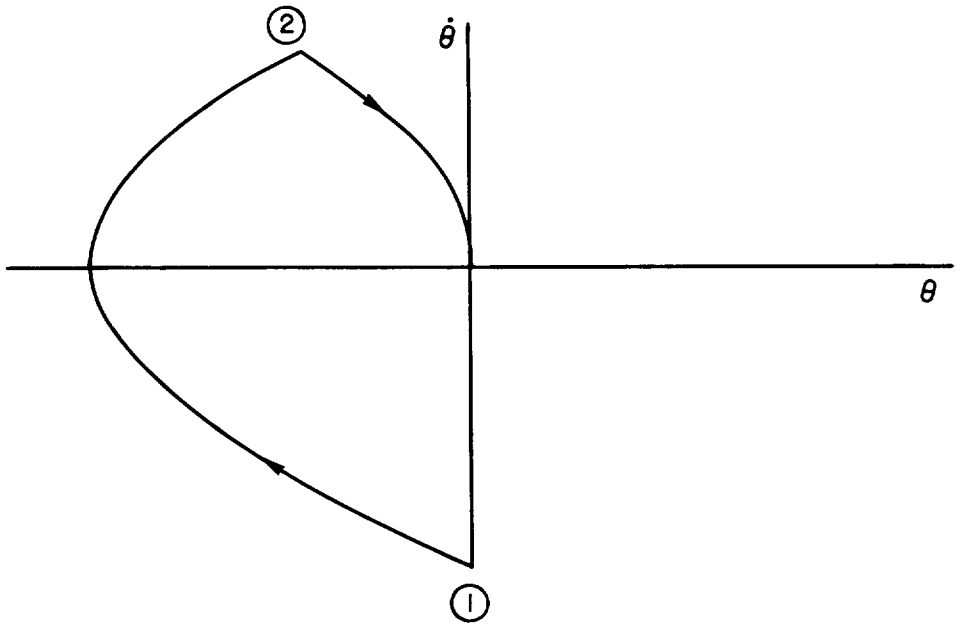

Sketch (k)

The angular rate is measured at point 1. Positive torque is then applied for a time $t_2 = \left(1 + \frac{\sqrt{2}}{2}\right)\frac{|\dot{\theta}_1|}{a}$. At point 2, negative torque is applied for $t_3 = \frac{\sqrt{2}}{2}\frac{|\dot{\theta}_1|}{a}$. The system is then at rest. The total settling time is

$$t_t = (1 + \sqrt{2})\frac{|\dot{\theta}_1|}{a} \tag{35}$$

while fuel consumption is simply

$$w_t = at_t = (1 + \sqrt{2})\,|\dot{\theta}_1| \tag{36}$$

Motions of the system for one cycle with unequal torques or rate measurement errors are shown in sketch (1).

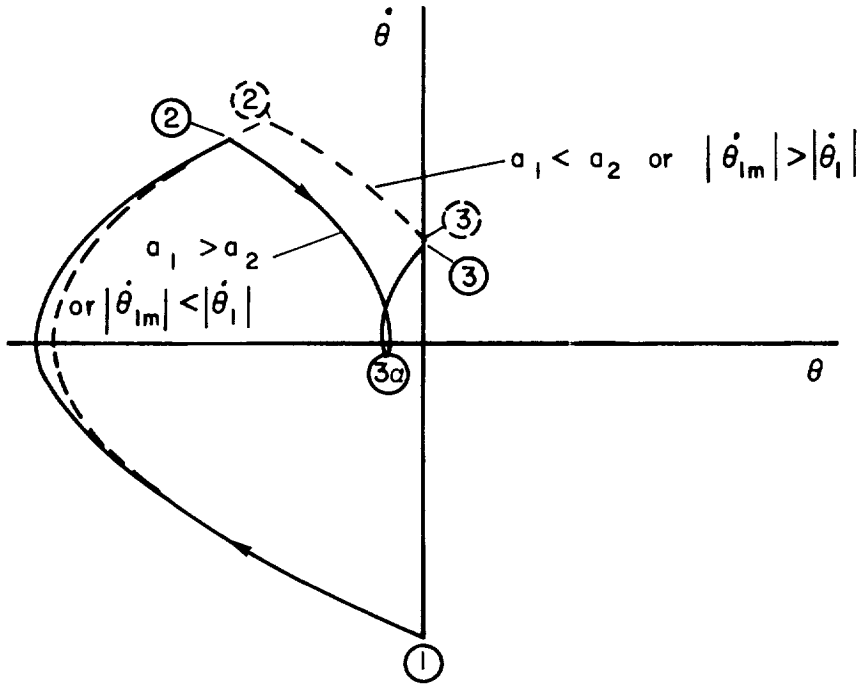

Sketch (1)

A rate measurement error $\dot{\theta}_{1m}$, or torque error will cause the vehicle to again overshoot or undershoot zero angle at the conclusion of the timed torque sequence. The equations including these effects for settling time and fuel consumption will now be given.

Case I, undershoot ($a_1 > a_2$ or $|\dot{\theta}_{1m}| < |\dot{\theta}_1|$): The vehicle does not reach zero error in the computed time sequence so positive torque is immediately applied to restore the error to zero. For an initial angular rate $\dot{\theta}_1$, the settling time for the first cycle can be expressed in dimensionless form as

$$\frac{at_c}{|\dot{\theta}_1|} = \frac{at_2}{|\dot{\theta}_1|} + \frac{at_{3\alpha}}{|\dot{\theta}_1|} + \frac{at_3}{|\dot{\theta}_1|} \tag{37}$$

where

$$\frac{at_2}{|\dot{\theta}_1|} = \left(1 + \frac{\sqrt{2}}{2}\right)\frac{\dot{\theta}_{1m}}{\dot{\theta}_1}$$

$$\frac{at_{3\alpha}}{|\dot{\theta}_1|} = \frac{\sqrt{2}}{2}\frac{\dot{\theta}_{1m}}{\dot{\theta}_1}$$

$$\frac{at_3}{|\dot{\theta}_1|} = -\frac{a}{a_2}\frac{\dot{\theta}_{3\alpha}}{\dot{\theta}_1} + \sqrt{\left(\frac{a}{a_2}\frac{\dot{\theta}_{3\alpha}}{\dot{\theta}_1}\right)^2 - \frac{2(\theta_{3\alpha} + \theta_d)a^2}{a_2\dot{\theta}_1^2}}$$

$$\frac{\dot{\theta}_{3\alpha}}{|\dot{\theta}_1|} = -1 + \left(1 + \frac{\sqrt{2}}{2}\right)\frac{a_2}{a}\frac{\dot{\theta}_{1m}}{\dot{\theta}_1} - \frac{a_1}{a}\frac{at_{3\alpha}}{|\dot{\theta}_1|}$$

$$\frac{a(\theta_{3\alpha} + \theta_d)}{\dot{\theta}_1^2} = \frac{a(\theta_2 + \theta_d)}{\dot{\theta}_1^2} + \frac{\dot{\theta}_2}{|\dot{\theta}_1|}\frac{at_{3\alpha}}{|\dot{\theta}_1|} - \frac{1}{2}\frac{a_1}{a}\left(\frac{at_{3\alpha}}{\dot{\theta}_1}\right)^2$$

$$\frac{\dot{\theta}_2}{|\dot{\theta}_1|} = -1 + \frac{a_2}{a}\frac{at_2}{|\dot{\theta}_1|}$$

$$\frac{a(\theta_2 + \theta_d)}{\dot{\theta}_1^2} = -\frac{at_2}{|\dot{\theta}_1|} + \frac{1}{2}\frac{a_2}{a}\left(\frac{at_2}{\dot{\theta}_1}\right)^2$$

The ratio of initial to final angular rates per cycle is

$$\frac{\dot{\theta}_3}{|\dot{\theta}_1|} = \frac{\dot{\theta}_{3\alpha}}{|\dot{\theta}_1|} + \frac{a_2}{a}\frac{at_3}{|\dot{\theta}_1|}$$

The torque-on time required to subside to a desired angular rate, $\dot{\theta}_d$, is

$$\frac{at_T}{|\dot{\theta}_1|} = \frac{at_c}{|\dot{\theta}_1|}\frac{1 - |\dot{\theta}_d/\dot{\theta}_1|}{1 - |\dot{\theta}_3/\dot{\theta}_1|} \tag{38}$$

The total settling time is

$$t_t = t_1 + \left(t_c + \frac{2\theta_d}{\dot{\theta}_d}\right)\frac{1 - |\dot{\theta}_d/\dot{\theta}_1|}{1 - |\dot{\theta}_3/\dot{\theta}_1|} \tag{39}$$

where

$$t_1 = \frac{\dot{\theta}_o}{a_1} + \sqrt{\left(\frac{\dot{\theta}_o}{a_1}\right)^2 + \frac{2\theta_o}{a_1}}$$

Fuel consumption is

$$w_t = \dot{\theta}_o + |\dot{\theta}_1| + w_c \frac{1 - |\dot{\theta}_1/\dot{\theta}_1|}{1 - |\dot{\theta}_3/\dot{\theta}_1|} \qquad (40)$$

where

$$w_c = |\dot{\theta}_1| + |\dot{\theta}_2| + 2|\dot{\theta}_{3\alpha}| + \dot{\theta}_3|$$

A4988

Case II, overshoot ($a_1 < a_2$ or $|\dot{\theta}_{1m}| > |\dot{\theta}_1|$): For an initial angular rate $\dot{\theta}_1$, the settling time for the first cycle is

$$\frac{at_c}{|\dot{\theta}_1|} = \frac{at_2}{|\dot{\theta}_1|} + \frac{at_3}{|\dot{\theta}_1|} \qquad (41)$$

where

$$\frac{at_3}{|\dot{\theta}_1|} = \frac{a}{a_1}\frac{\dot{\theta}_2}{|\dot{\theta}_1|} - \sqrt{\left(\frac{a}{a_1}\frac{\dot{\theta}_2}{\dot{\theta}_1}\right)^2 + \frac{2(\theta_2 + \theta_d)a^2}{a_1\dot{\theta}_1^2}}$$

The expressions for the remaining quantities in equation (41) are the same as for Case I. The ratio of initial to final angular rates per cycle is

$$\frac{\dot{\theta}_3}{|\dot{\theta}_1|} = \frac{\dot{\theta}_2}{|\dot{\theta}_1|} - \frac{a_1}{a}\frac{at_3}{|\dot{\theta}_1|}$$

Fuel consumption per cycle is

$$w_c = |\dot{\theta}_1| + 2|\dot{\theta}_2| - |\dot{\theta}_3| \qquad (42)$$

Total fuel consumption and settling times are found by substituting equations (41) and (42) into equations (39) and (40), respectively.

Limit-Cycle Characteristics

Fuel consumption.- Once a system with adequate settling time has been determined, the limit-cycle characteristics must be investigated to establish that the fuel consumption rate will be sufficiently low. The fuel consumption per second can be expressed in terms of the average change in angular velocity by the following equation which is analogous to equation (8)

$$W_{av} = \frac{Iw_{av}}{I_{sp}\tau_l} \tag{43}$$

where w_{av} is the average change in angular rate due to applied torque during limit-cycle motion.

With no external torque present, the average change in angular rate is determined by the torque-on time, which will be determined in a later section, and the width of the coast zone, θ_{co}. As will be shown subsequently, the limit cycle motion is symmetrical for a symmetrical linear switch curve system. In determining the fuel consumption rate, the total time will be approximated by the coasting time since the coasting time is much greater than the torque-on time. The average fuel consumption per second during limit-cycle motion can be expressed as

$$w_{av} = \frac{(a\tau_l)^2}{4\theta_{co}} \tag{44}$$

Hence the torque-on time, τ_l, should be as small as possible, while the coast zone, θ_{co}, should be as large as possible, consistent with tracking accuracy requirements.

In the presence of an external torque which is sufficiently large that a corrective pulse does not cause an overshoot of the dead zone on the opposite side, the fuel consumption is simply proportional to the acceleration produced by the external torque,

$$w_{av} = a_e \tag{45}$$

This amount of fuel would have to be expended even for a momentum exchange system, such as inertia wheels, in order to reduce the wheel speed periodically. For cases in which intermediate sized torques result in both dead zone boundaries being intercepted, the fuel consumption depends more on the particular system, and relations for general initial conditions at the dead-zone boundary are more difficult to obtain.

Torque-on time for system with linear switch curve.- The limit-cycle characteristics of the linear switch curve system are of particular interest since a linear switch curve could be used in conjunction with other systems in the low-amplitude limit-cycle range. The effects of hysteresis, time delays, time lags, and external torques on limit cycle characteristics will be investigated. The effects to be considered are shown in sketch (m).

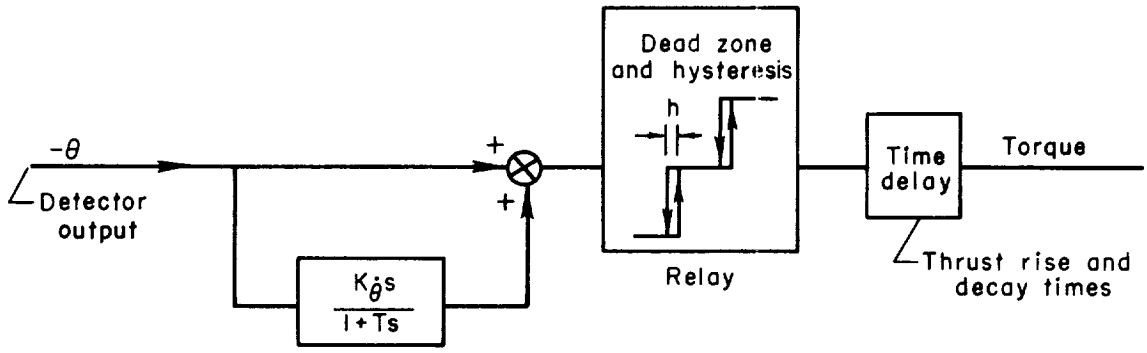

Sketch (m)

When a thrust-on signal is applied, a typical thrust transient response has the form indicated in sketch (n).

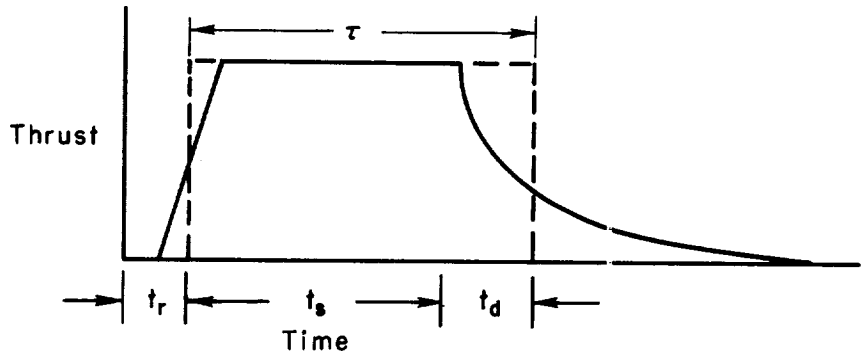

Sketch (n)

The thrust transient response has a rapid build-up and an exponential-type decay. The response can be approximated with sufficient accuracy by a step change in thrust and by the selection of time delays that keep the total area of the thrust-time curve the same. The time t_r is the delay, after the signal-on instant, before the step thrust is applied.

The time t_s represents the signal-on time after the step thrust is applied. The time t_d is the step thrust-on time representing the effect of thrust decay and thrust-off delay.

Typical motion near the limit-cycle condition without external torque is shown in sketch (o).

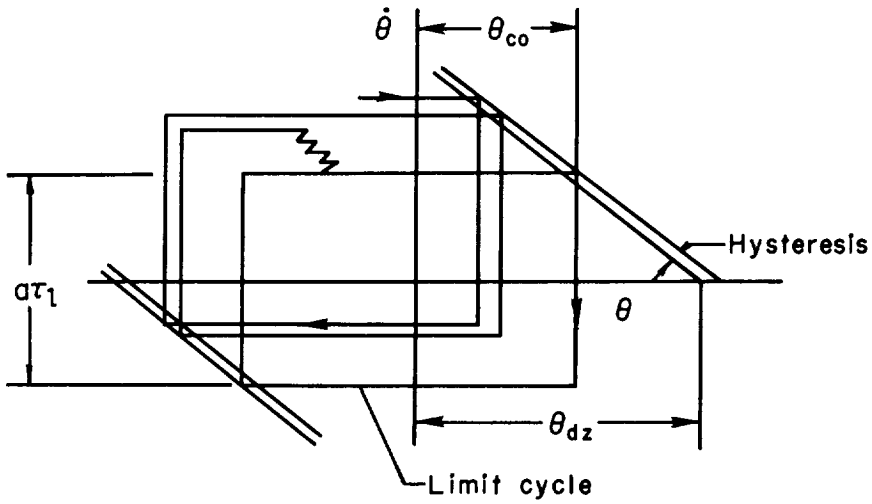

Sketch (o)

Since only small values of torque-on time will be considered, the parabolic torque-on trajectories approximate vertical straight lines. Although initially unsymmetric, the motion tends toward a symmetric limit cycle. It can be shown that the motion will converge to a symmetric limit cycle for sufficiently positive values of $K_{\dot{\theta}}$. This convergence is due to small changes in torque-on time with initial values of $\dot{\theta}$ at the switching boundary. The equations for torque-on time attributable to system imperfections will be given subsequently.

For the case with an external torque sufficiently large that only one switching boundary is reached, the motion becomes symmetrical only about the θ axis, but the same limit-cycle torque-on time occurs. For cases with intermediate values of torque, the torque-on time varies but it will be close to that corresponding to the limit cycle motion. Thus an estimate of the torque-on time for the limit cycle without an external torque gives a good indication of limit-cycle characteristics with an arbitrary value of external torque. A further discussion of limit cycles in the presence of external torque will be given in a subsequent section.

The coasting period is assumed sufficiently long for the signal from the differentiating network to reach a constant value equal to the

coasting angular velocity $\dot{\theta}_o$. For this initial condition, $\dot{\theta}_o$, the transient response of the output of the differentiating network, N(t), due to a negative step torque input is

$$N(t) = K_{\dot{\theta}} \left[\dot{\theta}_o - at + aT \left(1 - e^{-\frac{at}{aT}} \right) \right] \tag{46}$$

In the equations that follow, it will be convenient to combine the time parameters with the angular acceleration, a. The signal-on time after the torque is initially applied, t_s, (see sketch (n)) can be obtained from the following transcendental equation:

$$ah + at_r\dot{\theta}_o + at_s\dot{\theta}_o - \frac{(at_s)^2}{2} + aK_{\dot{\theta}} \left[aT \left(1 - e^{-\frac{at_s}{aT}} \right) - at_s \right] = 0 \tag{47}$$

The first two terms in equation (47) represent the change in control signal (sum of amplitude and differentiating network signals) required to initiate a cut-off signal. The remaining terms are the changes in the control signal while torque is applied. The total torque-on time, τ, is obtained by adding the thrust decay time to the signal-on time.

$$\tau = t_s + t_d \tag{48}$$

Equations (47) and (48) are used to determine the torque-on time which occurs for an arbitrary initial angular rate, $\dot{\theta}_c$, at the switch-curve boundary. The equations are valid for parameters for which torque-off occurs within the dead zone boundary. Two simplifications of equation (47) are of interest. For the first case with relatively large hysteresis and a small time constant, the exponential term can be neglected. After making this simplification and combining equations (47) and (48), the equation for torque-on time becomes

$$a\tau = \dot{\theta}_o - aK_{\dot{\theta}} + at_d + \left[(aK_{\dot{\theta}} - \dot{\theta}_o)^2 + 2ah + 2at_r\dot{\theta}_o + 2a^2K_{\dot{\theta}}T \right]^{\frac{1}{2}} \tag{49}$$

Results from this type of approximation were discussed in references 5 and 6. For the second case, which is of interest for this report, a relatively large time constant is used since a large value of $K_{\dot{\theta}}$ is desirable because of the low values of angular rate encountered. The large time constant is also useful in reducing effects of noise. When the signal-on time is short in comparison with the time constant, the exponential term in equation (47) can be expanded into a power series. By including the first three terms of the series, the following expression for torque-on time is obtained from equations (47) and (48).

$$aT = \frac{\left[\dot{\theta}_o^2 + 2(2ah + at_d\dot{\theta}_o)(1 + aK_{\dot{\theta}}/aT)\right]^{\frac{1}{2}}}{1 + aK_{\dot{\theta}}/aT} + at_d \tag{50}$$

The torque-on time for the limit-cycle motion, $a\tau_l$, can be obtained by use of the relation

$$a\tau_l = 2\dot{\theta}_o \tag{51}$$

After substituting equations (51) and (48) into equation (47), a transcendental equation for torque-on time for the limit-cycle case is obtained.

$$\frac{\tau_l}{2}(at_r + at_d) + ah - \frac{(at_d)^2}{2} - aK_{\dot{\theta}}\left[\tau_l - at_d - aT + aT\, e^{\left(\frac{at_d}{aT} - \frac{a\tau_l}{aT}\right)}\right] = 0 \tag{52}$$

Two approximate solutions of this equation can also be obtained. For the first case, with relatively large hysteresis and small time constants, equation (52) reduces to

$$\tau_l = \frac{2ah - (at_d)^2 + 2aK_{\dot{\theta}}(at_d + aT)}{2aK_{\dot{\theta}} - at_r - at_d} \tag{53}$$

For the present case with relatively large time constants, the exponential term in equation (52) is expanded into the first three terms of the power series and the resulting expression is

$$a\tau_l = at_d + (at_r + at_d)\frac{T}{2K_{\dot{\theta}}} + \left\{\left[at_d + (at_r + at_d)\frac{T}{2K_{\dot{\theta}}}\right]^2 - (at_d)^2\left(1 + \frac{T}{K_{\dot{\theta}}}\right) + \frac{2Tah}{K_{\dot{\theta}}}\right\}^{\frac{1}{2}} \tag{54}$$

Equation (54) indicates that the thrust rise time has a smaller effect on τ_l than the thrust decay time since $(T/K_{\dot{\theta}}) << 1$. If the thrust-rise time is approximated by the thrust decay time, equation (54) becomes

$$a\tau_l = at_d\left(1 + \frac{T}{K_{\dot{\theta}}}\right) + \left[\frac{(at_d)^2 T}{K_{\dot{\theta}}}\left(1 + \frac{T}{K_{\dot{\theta}}}\right) + \frac{2ahT}{K_{\dot{\theta}}}\right]^{\frac{1}{2}} \tag{55}$$

When the external torque is sufficiently large that the switch curve on only one side of the dead zone is encountered, the motion approaches a limit cycle with symmetry only about the θ axis. This motion will be discussed in more detail in a subsequent section. The previous equations for torque-on time can also be used in this case. The additional assumption is made that the effect of the small external

torque on the output of the differentiating network during the time that the torque is applied is negligible. An additional equation of interest for the case with external torque is the one for determining the torque-on time during limit-cycle motion which will just intersect both switching boundaries. The equation representing this limiting case of the intersection of the parabolic trajectory with the linear switch curve with a dead zone, θ_{dz}, is

$$a\tau_1 = - 2K_{\dot{\theta}}a_e + 4\sqrt{a_e\theta_{dz}} \tag{56}$$

RESULTS AND DISCUSSION

The predicted performance of the systems described in the previous section will be investigated. This will be done by a comparison of settling times and fuel consumption during recovery from the set of initial conditions described in sketch (a) in the previous section. In addition, limit-cycle characteristics (principally for the system with a linear switch curve) will also be discussed. Typical motions together with resulting fuel consumption rates will be shown. In subsequent calculated results, it will be convenient to show variables in a normalized form, based on the desired control accuracy, θ_d. The variables given in the previously derived equations in dimensional form were normalized to a unit value of desired tracking angle by dividing them by θ_d.

Recovery From Initial Errors

Linear switch-curve, minimum settling time, and rate-limited systems.- The performance of the systems with linear and nonlinear (minimum time) switch curves, and the rate-limited system are shown in figure 2. The linear and nonlinear switch curve systems will be discussed first. Typical phase plane motions for a specific level of acceleration are shown in figure 2(a). Similar curves were obtained for other acceleration levels and, for each acceleration, the value of $K_{\dot{\theta}}$ for the linear switch curve was adjusted to give a minimum average settling time for the range of initial conditions shown in figure 2(a). In making this adjustment, the nonlinear switch curve for the same value of acceleration was used as a guide. The linear switch curve system requires a longer settling time than the nonlinear switch curve system, although the difference in fuel consumption is relatively small (figs. 2(c) and 2(d)). The increase in time occurs principally during the latter part of the transient at low velocity levels and small average applied torques. At these low velocities, the linear system produces an exponential decrease in velocity with time with a decreasing average value

of torque, while the nonlinear system produces a linear decrease in velocity with full torque applied in one direction. For a settling time of about one minute, approximately 30 percent more fuel must be expended by the linear system than by the nonlinear system. The larger values of acceleration allow shorter settling times but require more fuel. Also, if very large accelerations were considered, fuel consumption during limit-cycle operation would become too great when effects of imperfections such as time delays were included. These limit-cycle characteristics will be discussed in a later section.

As an example of the weight of the fuel required to recover from an initial error for a typical case, consider a vehicle with $I = 10^{10}$ gm cm^2, $l = 75$ cm, a desired tracking accuracy of $\theta_d = 0.1$ second of arc, and a relatively low efficiency fuel, such as water vapor, for which $I_{sp} = 50$ seconds will be assumed. Note that for an acceleration of $3\theta_d/\text{sec}^2$, a total thrust of only about 200 dynes is required. After a typical value of $\bar{w}_t/\theta_d = 120/\text{sec}$ is selected, I_{sp} is converted to cgs form, and these values are substituted into equation (8), a weight of 0.158 gm is obtained. If this correction is required once every other 100 minute orbit about each of two axes for one year, a total of 830 grams of fuel would be expended.

Typical phase plane trajectories for the rate-limited system are shown in figure 2(b). For a given settling time, the fuel consumption can be considerably reduced by the use of rate limiting. The rate signal could be produced by either a lead network operating from the detector signal, or from a separate source such as a rate gyro if the rates are sufficiently large.

An important effect to be considered is saturation of the detector since a large error range of 1000 to 1 is desired. The detector output is a signal assumed proportional to error angle. However, at some value of error input, the detector may saturate and its output will be limited at this value for increasing error angles. If a lead network is assumed for rate information, error rate is also only available when the detector is operating within its proportional limits. The effect of detector error saturation on the performance of the linear and nonlinear switch curve systems is shown in figure 3. In the determination of the linear switch curves, the values of $K_{\dot{\theta}}$ selected were those which gave minimum time response for the error and error rate range of interest below each error limit value. A large increase in settling time and fuel consumption occurs as detector saturation limits become lower. For the lower values of detector saturation, there is little difference in performance between the two systems since most of the time and fuel is utilized in recovering to within the proportional range of the detector. With a detector limit of $\theta_L/\theta_d = 50$, a three minute settling time can still be achieved for the acceleration range shown. However, fuel consumption has increased by a factor of about five from

the unsaturated case to 4,300 grams. For a detector saturation of $\theta_L/\theta_d = 100$, the fuel required for the system to settle within three minutes is reduced to about 2,300 grams. Hence, a detector range of at least 50 θ_d to 100 θ_d would be required. For an application such as the orbiting astronomical observatory, this range may be difficult to obtain since problems of alinement dictate that the error signal be obtained from the primary optical system.

Timer systems.- Two systems which can operate with a minimum detector range will now be discussed. In both cases, a high resolution timer is used to apply a timed sequence of torques, open loop, between measuring intervals. The timer accuracies depend upon the residual angular velocity desired, and could be as high as 10 milliseconds. The effects of torque magnitude errors will be discussed. As a limit cycle condition is approached, a second mode of operation generally must be used. Otherwise the requirements on system lags, etc., would become too stringent.

The performance of the first timer system which requires only the direction of error from the detector is shown in figures 4 and 5. The system operates as shown in figure 4(a). The time required to move from condition 1 $(0, \dot{\theta}_1)$ to condition 2 with positive torque applied is measured. Then opposite torque is applied for 85.3 percent of the first measured time. Then positive torque is applied again for 35.3 percent of the original measured time. If the applied torques in each direction are symmetrical, then final switching occurs as shown by the nonlinear switch curve in figure 2(a), and the vehicle is returned to rest. However, if negative torque is greater than positive torque ($a_1 > a_2$), the trajectory tends to overshoot the origin of the phase plane and the angular rate is too large when zero angle is reached. One cycle of the motion is completed. The cycle is then repeated until the measured timed interval is small enough to indicate that the angular rate is reduced to a desired level. Note that quite accurate time resolution would be required as a limit cycle condition is approached. If negative torque is less than positive torque, undershoot occurs at the end of the 35.3 percent time interval, and negative torque is then applied until zero angle is reached. The cycle is then repeated.

The ratio of final velocity to initial velocity for each cycle, $\dot{\theta}_4/\dot{\theta}_1$, is a function of the torque error (fig. 4(b)). For torque errors greater than ±7.9 percent from the average value for the $a_1 > a_2$ case, and torque errors greater than 11.5 percent for the $a_1 < a_2$ case, $|\dot{\theta}_4|$ becomes greater than $|\dot{\theta}_1|$ and the system is unstable. The variation of time per cycle with torque error is shown in figure 4(c) and is seen to be fairly small. The effect of torque error on total settling time with $\dot{\theta}_d = \theta_d = 0$ is shown in figure 4(d). A large increase in settling time with increasing torque error is indicated.

For a comparison with the previous systems, the performance of the timer system was computed for the previous set of initial conditions (fig. 5) through use of equations (26) and (27) with $\dot{\theta}_d/\theta_d = 0.25$ and $\theta_d = 1$. The values shown for a given percent torque asymmetry represent the arithmetic average of the $a_1<a<a_2$ and $a_1>a>a_2$ relative torque cases. When compared with figure 3, the settling time and fuel consumption of the timer system without thrust error are seen to be approximately equivalent to the linear switch-curve system with detector limiting of about $150\ \theta_L/\theta_d$. With a ±2 percent thrust error, the performance is equivalent to the linear switch-curve system with about $50\ \theta_L/\theta_d$ detector limiting. Hence the timer system becomes competitive only for low values of detector limiting.

For large thrust errors it becomes more efficient to apply corrective thrust only when the error returns to the same sign that existed when the time measurement was made. This modified system is shown in figure 6. A comparison with figure 4(d) indicates that while the time required by the modified timer system for the symmetrical thrust case is almost twice that of the timer system, the total time becomes equal or less when the thrust error becomes ±1.5 percent or greater.

The results for the second timer system to be called the rate system are shown in figures 7, 8, and 9 with a typical trajectory shown in figure 7(a). The rate $\dot{\theta}_1$ is measured at $\theta = 0$ by use of a lead network. Positive torque is then applied for $1.706\ \theta_1/a$ seconds. Then negative torque is applied for $0.706\ \dot{\theta}_1/a$ second and the vehicle is returned to equilibrium. For symmetrical torques, final switching occurs at the conditions given by the nonlinear switch curve (fig. 2). Accurate time resolution is also needed for this case. For unsymmetrical torques, the vehicle is not returned to equilibrium but will tend to either overshoot or undershoot (fig. 7(a)) in a manner similar to the timer system and the cycle must then be repeated. The rate system produces a much smaller rate error per cycle ($\dot{\theta}_3$) than the timer system for a given torque error. This difference results largely from a smaller error in the final switching instants (figs. 4(a) and 7(a)). In addition to inaccuracies in torque magnitude, this system would also be subject to inaccuracies in rate measurement by the lead network (fig. 8). A comparison with the effects of torque error shows that a given percentage of rate measurement error causes a slightly greater increase in average settling time than the same percentage of torque error (figs. 7(d) and 8(d)).

The performance of the rate system in recovering from the previous set of initial conditions (fig. 9) was calculated through use of equations (39) and (40) with $\dot{\theta}_d/\theta_d = 0.25$ and $\theta_d = 1$. The values shown for a given percent torque asymmetry represent the arithmetic average of the $a_1<a<a_2$ and $a_1>a>a_2$ relative torque cases. A comparison with the linear switch curve system (fig. 3) indicates that without torque error, the

rate system performance was approximately equivalent to the linear switch-curve system with detector saturation of $\theta_L/\theta_d = 200$. With a ±2 percent torque error, the rate system performance was roughly equal to the linear switch curve system with detector limiting of $\theta_L/\theta_d = 100$.

Limit-Cycle Characteristics

For any of the previously discussed systems, the limit-cycle characteristics must be investigated to see if a stable limit cycle exists and if fuel consumption is sufficiently low. The characteristics of a system with a lead network will be investigated primarily. The network could be used with any of the previously discussed systems since a proportional error signal would be available during motions close to limit-cycle conditions.

Linear switch-curve system.- The influence of lead network parameters, hysteresis effects, and time delays on limit cycle performance for an on-off system with linear switch curve will be investigated. Typical motions near the limit cycle with different amounts of external torque present are shown in figure 10. With no external torque (fig. 10(a)), the motion shifts toward a symmetrical limit cycle asymptotically. With an external torque sufficiently large so that only one switch curve is encountered (fig. 10(b)), the motion shifts toward a limit cycle which is symmetrical only about the θ/θ_d axis. For intermediate values of torque (fig. 10(c))for which both switch curves are intersected, a true limit cycle is not attained, but the motion gradually hunts back and forth within a region determined by the switch curves. The time intervals during which torque is applied near a limit-cycle condition will be referred to as torque-on times. Since these times are very small, the parabolic torque-on trajectories approximate vertical straight lines. The variations in torque-on time near the limit cycle cycle are seen to be very small and they approach the same value for the limit cycles shown in figures (10a) and (10b).

The selection of torque-on time for the limit cycle motion depends upon the magnitude of external torque expected. As stated in the analysis section, fuel consumption for the motion shown in figure 10(b) depends only on the magnitude of the external torque. Hence it would be desirable to make the torque-on time as small as possible so that only one switch curve would be intercepted (fig. 10(b)) for a wide range of external torques, and therefore any fuel expended would be used only in counteracting the external torques. However, a smaller torque-on time for a limit cycle places more stringent requirements on system imperfections, such as hysteresis and time lags. Typical variations in torque-on times for a limit cycle for cases with large time constants in the lead network (eq. (55)) are shown in figure 11.

As a compromise between these conflicting requirements, suppose for the example in figure 10 that a sufficiently small torque-on time is selected so that only one switch curve is encountered with external disturbances present as low as 0.005 θ_d/sec^2. The other system constants for the figure (10) example are $K_{\dot{\theta}} = 5.0$, $\theta_{dz}/\theta_d = 1.5$. Then, from equation (56), a normalized torque-on time, $a\tau_l$, not greater than 0.29 θ_d/sec should be used. From the previous discussion on recovery from initial errors, a typical value of applied acceleration is 2.5 θ_d/sec^2. Hence, the firing interval required is about 0.1 second. To achieve this pulse increment with the given value of acceleration, quite stringent requirements are placed on values of time lags and hysteresis. For instance, for $K_{\dot{\theta}}/T = 10$, a combination of hysteresis of 0.08 θ_d and a time delay of 0.032 second would be needed to achieve the desired pulse size. An additional effect to be considered in the selection of the dead zone is that, although only angular tracking accuracy is required, the linear switch curve will produce switching at different values of angular error, depending on the amount of angular rate present (fig. 10). This variation is particularly troublesome for motions with intermediate amounts of external torque present (fig. 10(c)). Hence, the switch curve dead zone should be selected so that θ_{co} (sketch (o)) during limit cycle motion (without an external torque present) is somewhat less than the desired tracking accuracy, θ_d. This reduction in dead zone increases the fuel consumption for cases with zero or very small amounts of external torque.

An estimate of the weight of the fuel consumed during the limit-cycle motion can be made for the previous example of $I = 10^{10}$ gm cm^2, $I_{sp} = 50$ seconds, $l = 75$ cm, and $\theta_d = 0.1$ second of arc. If an acceleration of 0.02 θ_d per sec^2 due to an external torque is present, then the resulting fuel consumption (eqs. (45) and (43)) is $W_{av} = 2.63\times10^{-5}$ gm/sec. The total fuel required for continuous two-axis control for a year for these assumed conditions would be 1650 grams. If no external torque is assumed, $\theta_{co} = 0.09$ second of arc, and $a\tau_l = 0.29\ \theta_d$ then the resulting average fuel consumption (eqs. (44) and (43)) is $W_{av} = 3.09\times10^{-5}$ gm/sec.

Incremental control system.- The performance of an alternate system for a case for which the angular rate becomes too small to obtain an adequate rate signal is shown in figure 12. In addition, this system can be used with dead zone values closer to the desired tracking angular value since the tracking angle at which the pulse is fired does not depend upon angular rate. This incremental-type system uses pulses of fixed magnitude applied at discrete angle increments. To cope with the

effects of external torques, and still use a desired angle increment and pulse size, a memory of the two previous angle increments is required. As shown in the figure, a single pulse is applied at each angle increment that is of greater absolute magnitude than the previous one. If the same angle is reached again after a single pulse is applied, then a double pulse is used (fig. 12(b)). (For the $\theta/\theta_d = 1$ value, only single pulses are used). For both the time histories shown, the settling time was fairly long (about 1-1/2 minutes). Note that if the incremental system is combined with the previously discussed on-off linear switch curve system, the limit-cycle torque-on time for the latter system must still be determined to insure that the resulting pulse is of the same order of magnitude as the fixed pulse.

CONCLUSIONS

The performance of several systems using on-off reaction jets for precision attitude control of a satellite has been investigated. Both effects of recovery from large disturbances and of limit-cycle characteristics have been included.

1. Detector saturation was found to have a major influence on settling time and fuel-consumption characteristics for the example considered. For a lead network system, a detector range of at least 50 to 100 times desired tracking accuracy was required to give satisfactory values of settling time and fuel consumption.

2. Rate limiting was an attractive way to reduce fuel consumption and still obtain a specified settling time. When a lead network was used, no signal was available during detector saturation. Hence an auxiliary source of rate signal for limit detection would be needed.

3. The performance of a system designed for use with a minimum detector range by means of a timed sequence of torques was also investigated. This system required a high resolution timer of up to 10 milliseconds accuracy. Although this system required a longer settling time and higher fuel consumption rate than the lead network system without detector saturation present, it achieved better performance than the lead network system with low detector saturation values. However, differences in positive and negative applied torque levels were found to have a large effect on settling time and fuel consumption of the timer system; for example, for a torque difference of ±2 percent, settling time was doubled.

4. Another system which used a combination of a timer and a rate measurement only during motion over a small detector range achieved settling times about one half of those for the timer system.

5. Fuel consumption was low during limit-cycle operation of a system with a linear switch curve, and realistic values of hysteresis, lead network constants, dead zone, and thrust time delays, provided the applied torque level was moderate.

Ames Research Center
National Aeronautics and Space Administration
Moffett Field, Calif., May 9, 1961

APPENDIX

DERIVATION OF EQUATIONS FOR SETTLING TIME AND FUEL CONSUMPTION FOR LINEAR SWITCH-CURVE SYSTEM

As stated in the analysis section, the motion for this system (sketch (c)) may be separated into three parts:

(1) The time required to reach the switch curve initially from a given set of initial conditions,

(2) The time required during which the trajectory overshoots the switch curve when it is intersected, and

(3) The time during which the motion subsides along the switch curve until the desired attitude angle is reached.

The time for the first part of the motion can be determined through use of the equations for the switch curve and the trajectory segment

$$t_1 = \frac{\dot{\theta}_0}{a} - K_{\dot{\theta}} + \sqrt{K_{\dot{\theta}}^2 + \left(\frac{\dot{\theta}_0}{a}\right)^2 + \frac{2\theta_0}{a}} \qquad (A1)$$

The angular rate at the first intersection of the switch curve is

$$\dot{\theta}_1 = \dot{\theta}_0 - at_1 \qquad (A2)$$

For the second part of the motion, there are a series of trajectory segments which start and terminate at the switch curve. The time required for the nth trajectory segment can be expressed in terms of the angular rate at the beginning of the trajectory segment as

$$t_n = -2K_{\dot{\theta}} + \left| \frac{2\dot{\theta}_{n-1}}{a} \right| \qquad (A3)$$

with $n \geq 2$. The equation for $\dot{\theta}_n$ at the end of the nth trajectory segment is

$$\left| \dot{\theta}_n \right| = \left| -\dot{\theta}_1 - 2aK_{\dot{\theta}}(n-1) \right| \qquad (A4)$$

with $n \geq 1$. For a given value of $\dot{\theta}_1$ which corresponds to the first intersection of the trajectory with the switch curve, the total time for motions represented by n-1 trajectory segments can be obtained by combining equations (A3) and (A4)

$$t_n = \left(6K_{\dot{\theta}} - \frac{2\dot{\theta}_1}{a}\right)(N - 1) - 4K_{\dot{\theta}} \sum_{n=2}^{N} n \qquad (A5)$$

The total number of segments, N, is determined by the requirement that the motion be reduced to small enough values so accelerations commanded by the switch curve will be within the acceleration capability of the vehicle. Geometrically, this condition occurs when the magnitude of the slope of the phase-plane trajectory is equal to or greater than the magnitude of the slope of the switch curve. The maximum angular rate for which this occurs is

$$|\dot{\theta}| = aK_{\dot{\theta}} \qquad (A6)$$

If equations (A6) and (A4) are combined, N is seen to be the integral value of n for which the following relation holds

$$\left| -\dot{\theta}_1 - 2aK_{\dot{\theta}}(n-1) \right| \leq aK_{\dot{\theta}}$$

or N is the nearest integral value of $(-\dot{\theta}_1/2aK_{\dot{\theta}}) + 1$.

Part three of the motion is the average motion that is commanded by the switch curve. A sufficiently wide dead zone along the switch curve is assumed so that corrective torque is applied intermittently in only one direction to reduce the angular rate to zero. Hence, the time-averaged value of torque is less than the steady torque-on value. The resulting average motion is described by a linear first-order differential equation with a root equal to $-1/K_{\dot{\theta}}$. After equation (A4) is used to determine the initial angular rate for this motion, $\dot{\theta}_N$, and with the given desired tracking angle, θ_d, the third portion of the settling time, t_L, is determined by the equation

$$t_L = K_{\dot{\theta}} \log_e \left| \frac{1}{\theta_d} \left[-K_{\dot{\theta}}\dot{\theta}_1 - 2aK_{\dot{\theta}}^2(N - 1) \right] \right| \qquad (A7)$$

where $\log_e |\ \ | = 0$ if $|\ \ | < 1$. The total settling time is given by the sum of equations (A1), (A5), and (A7).

$$t_t = t_1 + \left(6K_{\dot{\theta}} - \frac{2\dot{\theta}_1}{a}\right)(N - 1) - 4K_{\dot{\theta}} \sum_{n=2}^{N} n + K_{\dot{\theta}} \log_e \left| \frac{1}{\theta_d} \left[-K_{\dot{\theta}}\dot{\theta}_1 - 2aK_{\dot{\theta}}^2(N - 1) \right] \right| \qquad (A8)$$

In determining fuel consumption, the total number of switchings must be defined differently than for the settling time case since fuel consumption depends only on the summation of maximum velocities obtained. As shown by the trajectory which starts at θ_o^*, $\dot{\theta}_o^*$ in sketch (c), the last two switchings may occur with the same sign of $\dot{\theta}$ and hence the final switching should be excluded for this type of trajectory. This effect can be included through use of equation (A4) and by defining the final trajectory segment N′ as the minimum value of n for which

$$-\dot{\theta}_1 - 2aK_{\dot{\theta}}(n - 1) < 2aK_{\dot{\theta}}$$

or N′ is the nearest integral value of $(-\dot{\theta}/2aK_{\dot{\theta}}) + 0.5$. The normalized fuel weight is calculated from the sum of the angular rate changes.

$$w_t = \dot{\theta}_o + 2\sum_{n=1}^{N'} |\dot{\theta}_n| \tag{A9}$$

After the substitution of equations (A4) into equation (A9), the following expression is obtained.

$$w_t = \dot{\theta}_o + 2N'(2aK_{\dot{\theta}} - \dot{\theta}_1) - 4aK_{\dot{\theta}} \sum_{n=1}^{N'} n \tag{A10}$$

REFERENCES

1. Triplett, William C.: Design Considerations for an Orbiting Astronomical Observatory. ARS Preprint 1184-60, 1960.

2. Roberson, Robert E.: Attitude Control of a Satellite Vehicle - An Outline of the Problems. ARS Preprint 485-57, 1957.

3. Frye, William E., and Stearns, Edward V.: Stabilization and Attitude Control of Satellite Vehicles. ARS Jour., vol. 29, no. 12, Dec. 1959, pp. 927-931.

4. White, John S., and Hansen, Q. Marion: Study of Systems Using Inertia Wheels for Precise Attitude Control of a Satellite. NASA TN D-691, 1961.

5. Pistiner, Josef S.: On-Off Control System for Attitude Stabilization of a Space Vehicle. ARS Jour., vol. 29, no. 4, April 1959, pp. 283-289.

6. Freeman, George W.: Limit-Cycle Efficiency of On-Off Reaction Control Systems. IAS National Specialists Meeting on Guidance of Aerospace Vehicles, Boston, Mass., May 1960, pp. 84-97.

7. Flügge-Lotz, Irmgard and Lindberg, Herbert E.: Studies of Second- and Third-Order Contactor Control Systems. NASA TN D-107, 1959.

8. Tsien, H.S.: Engineering Cybernetics. McGraw-Hill Book Co., 1954.

9. Cunningham, W. J.: Introduction to Nonlinear Analysis. McGraw-Hill Book Co., 1958.

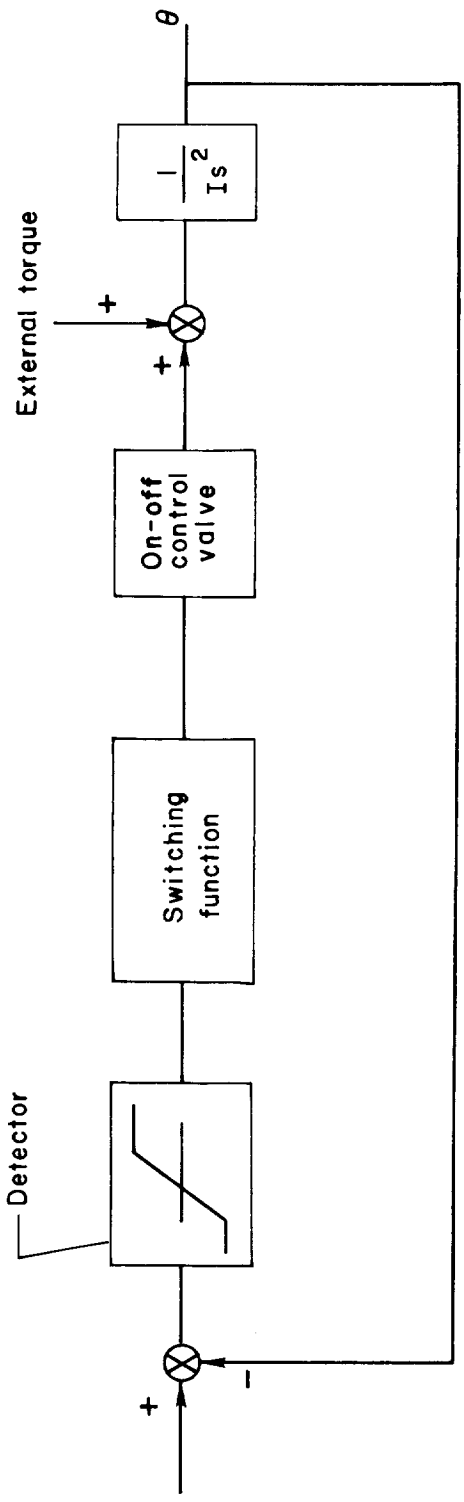

Figure 1.- Block diagram of on-off control system.

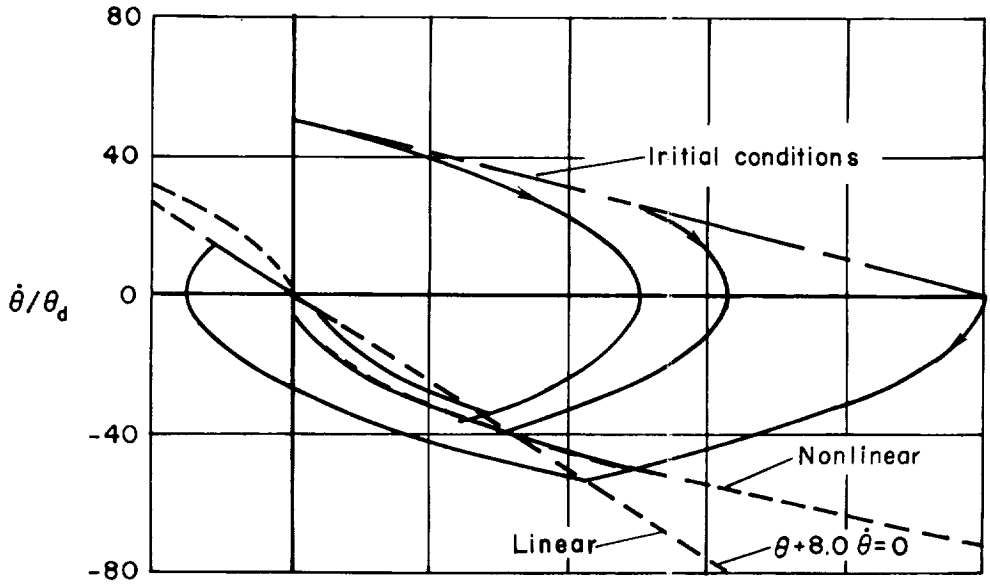

(a) Typical phase plane trajectories for minimum time linear and nonlinear switch curve systems.

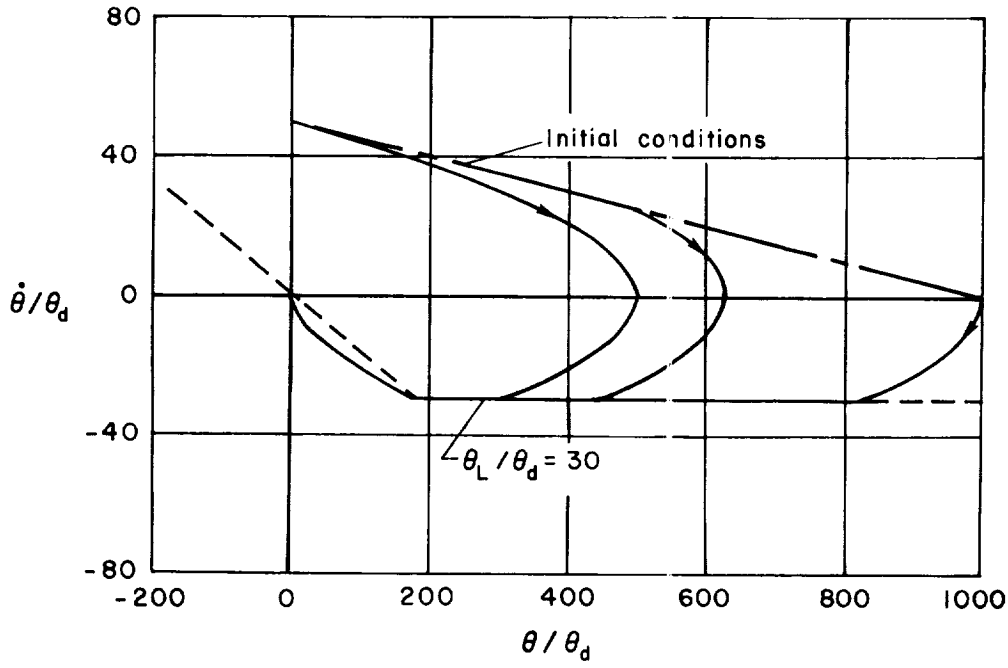

(b) Typical phase plane trajectories for rate-limited system.

Figure 2.- Comparison of minimum settling time linear and nonlinear switch curve systems, and rate-limited system.

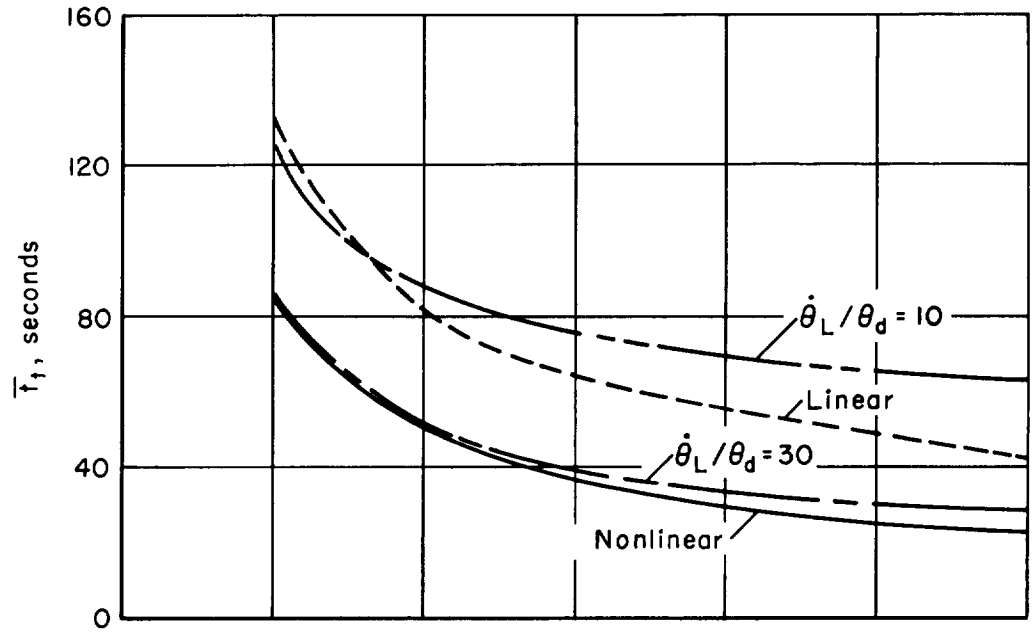

(c) Settling time.

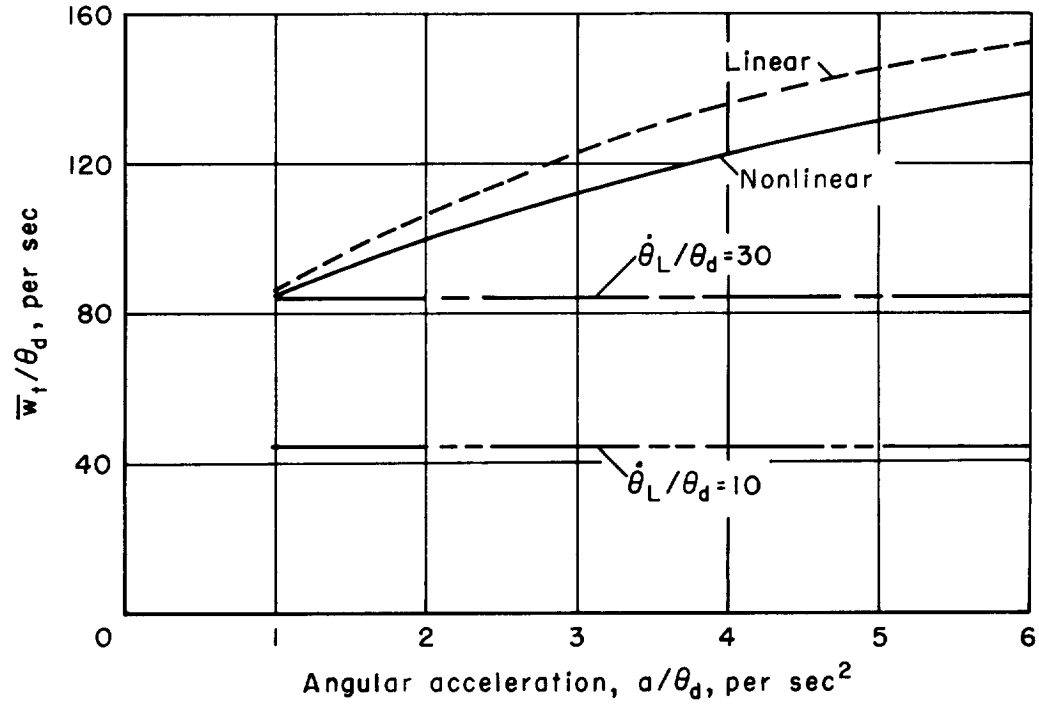

(d) Relative fuel consumption.

Figure 2.- Concluded.

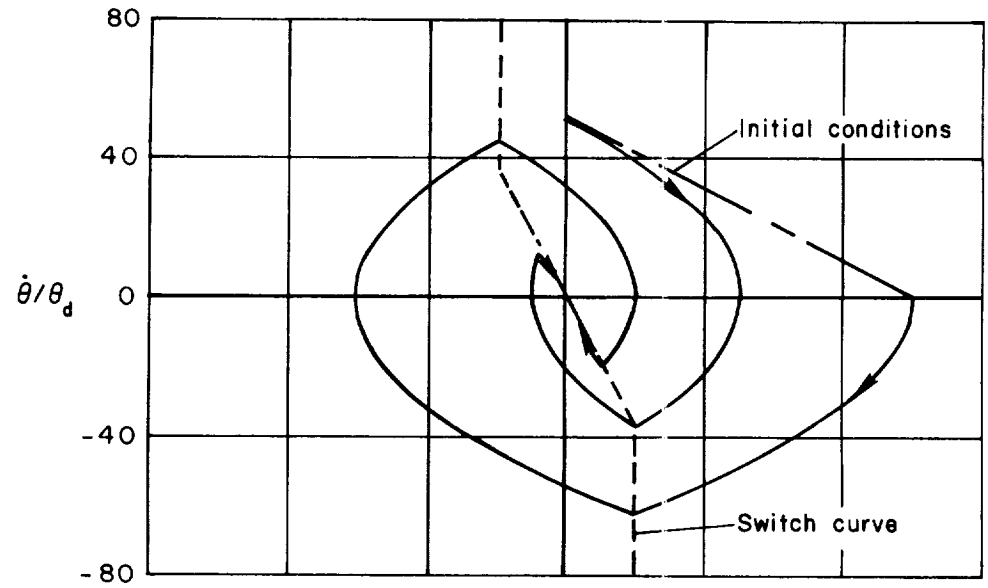

(a) Typical phase plane trajectory for amplitude limit of $\theta_L/\theta_d = 200$.

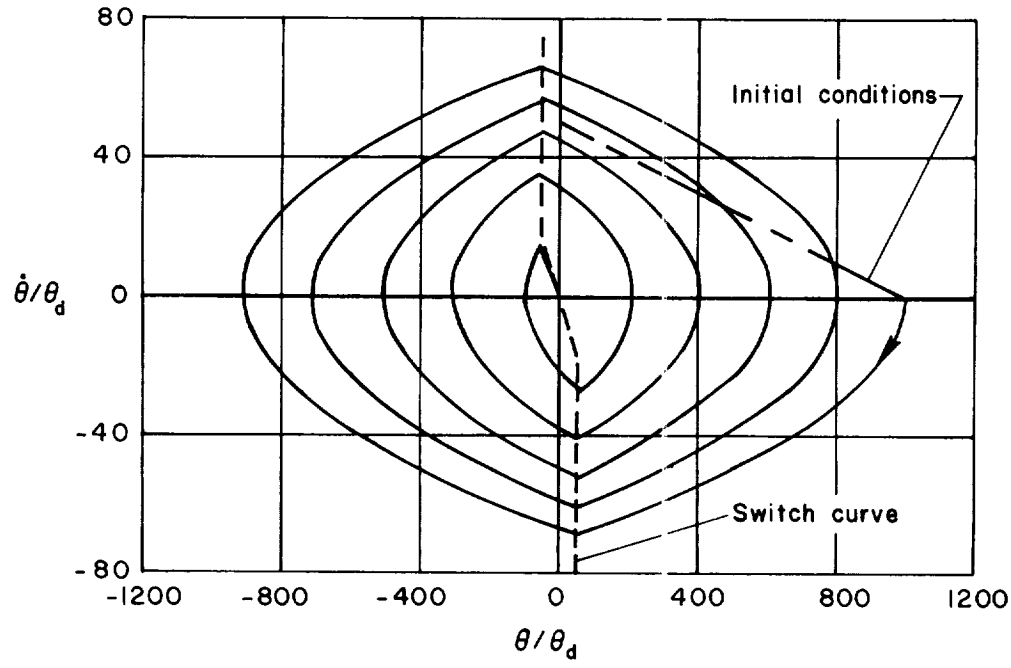

(b) Typical phase plane trajectory for amplitude limit of $\theta_L/\theta_d = 50$.

Figure 3.- Effect of detector saturation on minimum settling time linear and nonlinear switch curve systems.

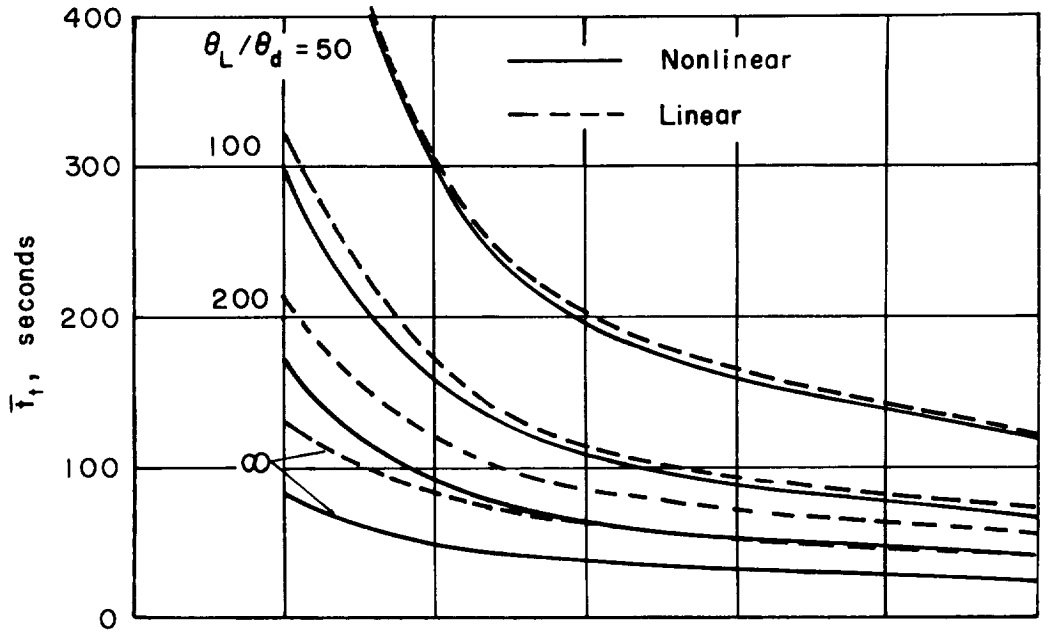

(c) Settling time.

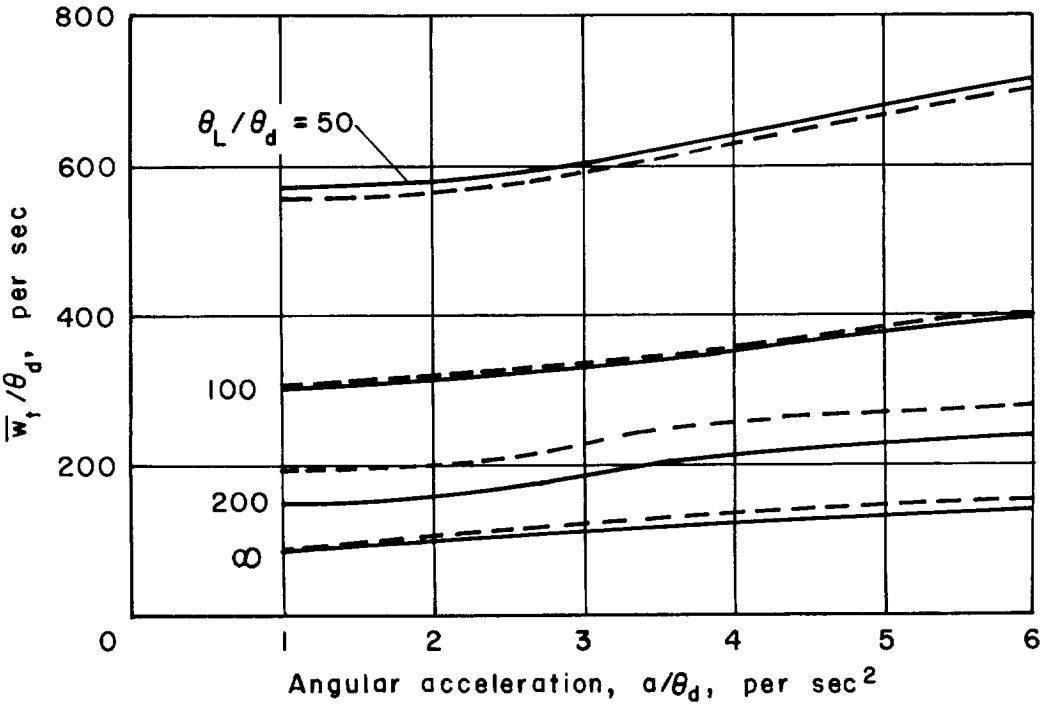

(d) Relative fuel consumption.

Figure 3.- Concluded.

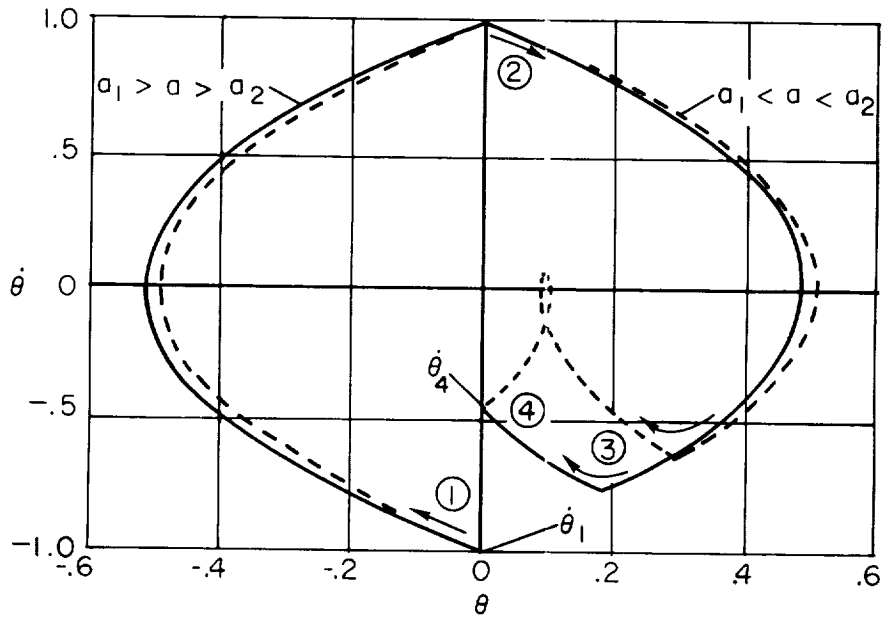

(a) Normalized phase plane trajectory; torque error = ±2 percent.

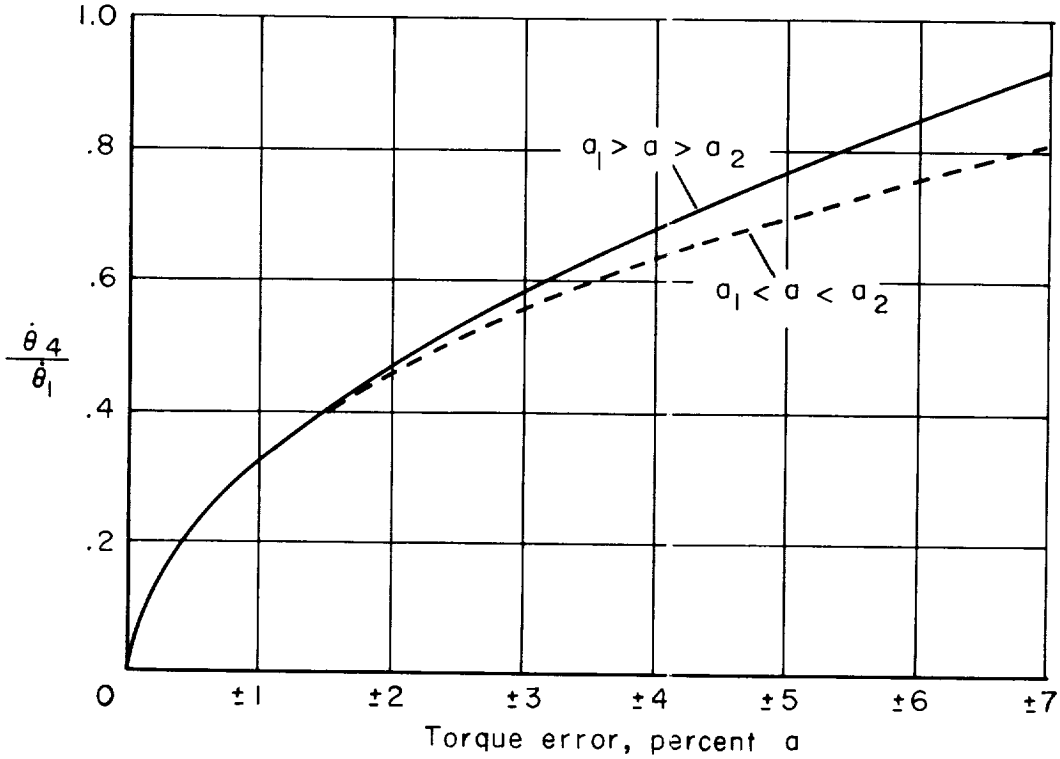

(b) Velocity decrement, per cycle.

Figure 4.- Effect of torque error on timer system response.

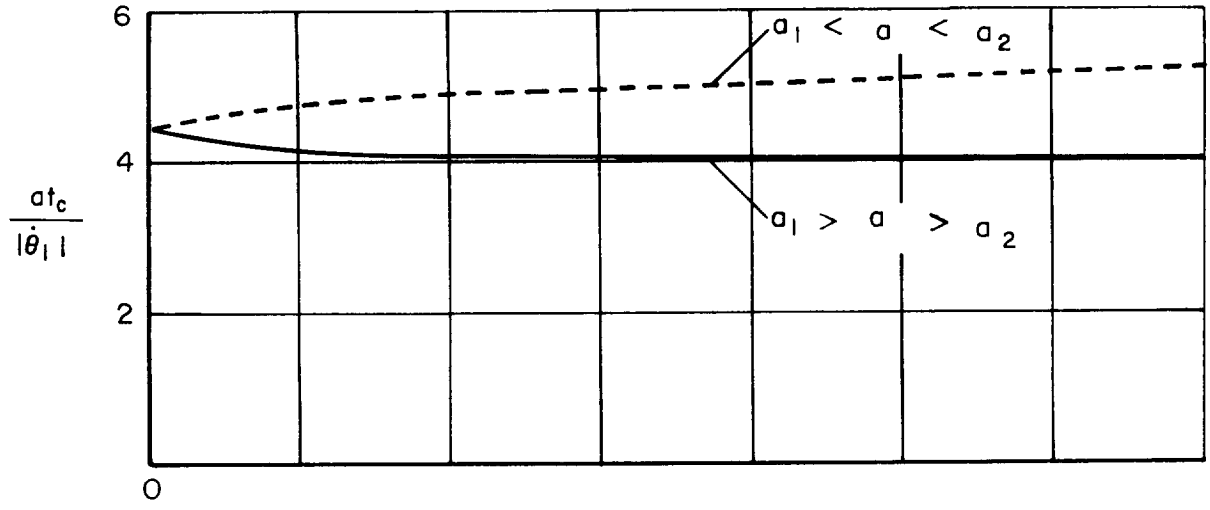

(c) Time, per cycle.

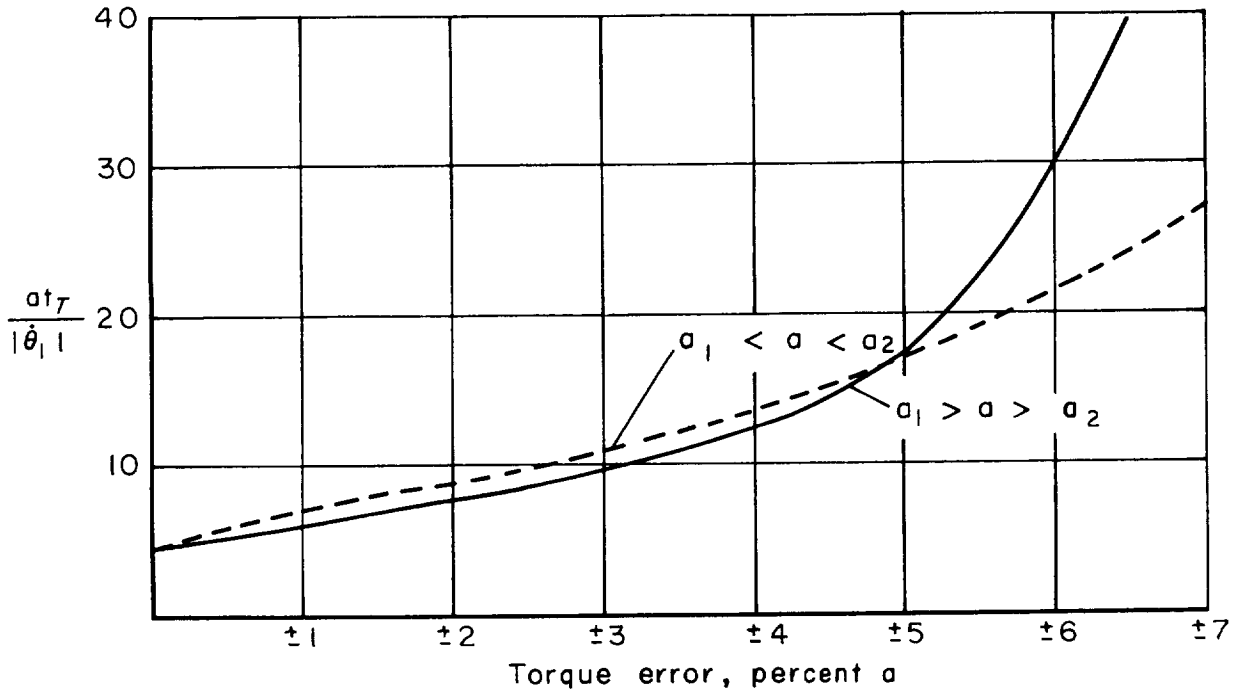

(d) Total settling time for an initial rate error.

Figure 4.- Concluded.

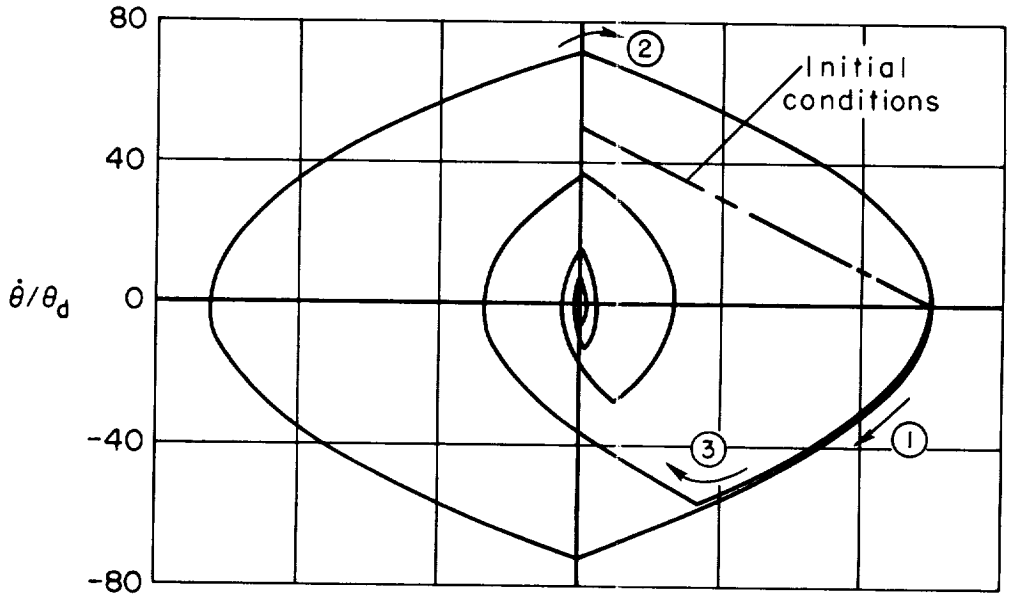

(a) Typical phase plane trajectory; a_1/a_2 = 1.02/0.98.

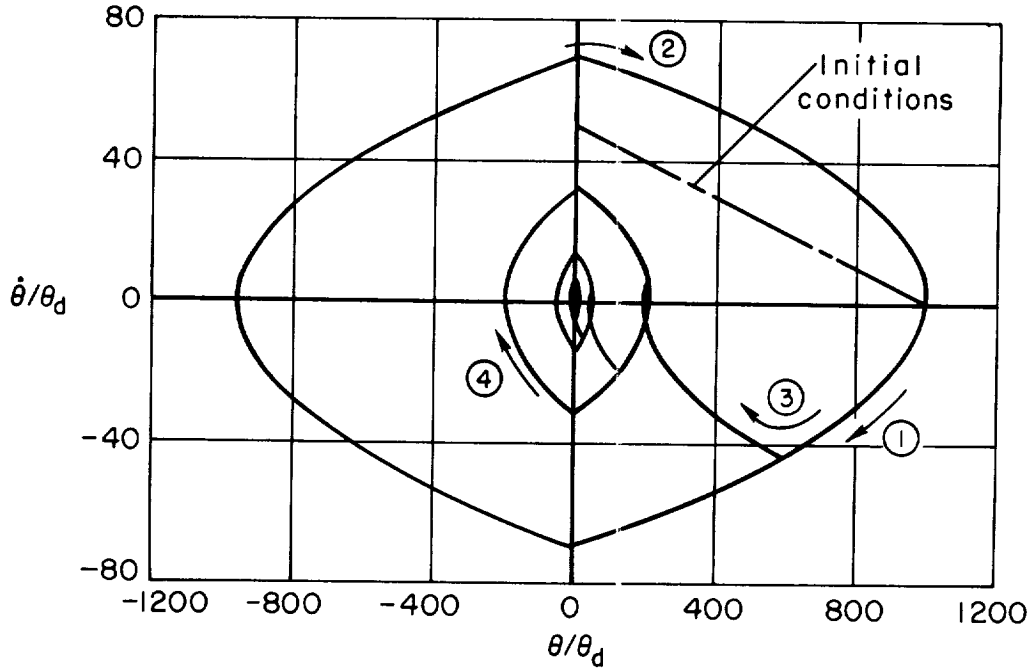

(b) Typical phase plane trajectory; a_1/a_2 = 0.98/1.02.

Figure 5.- Effect of torque error on timer system response to initial conditions.

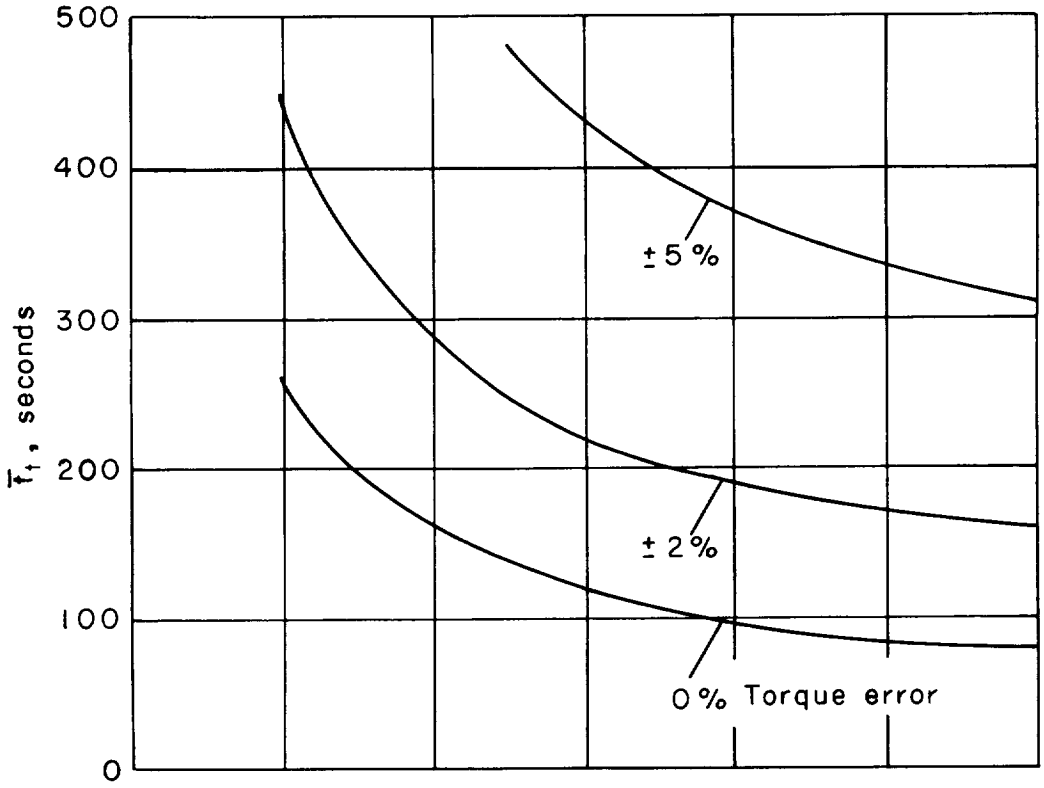

(c) Settling time.

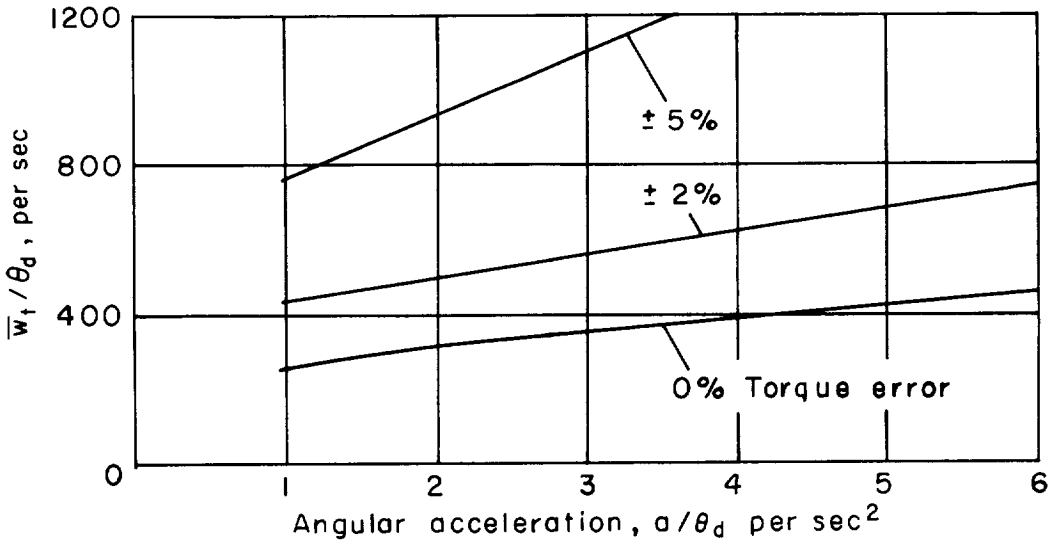

(d) Relative fuel consumption.

Figure 5.- Concluded.

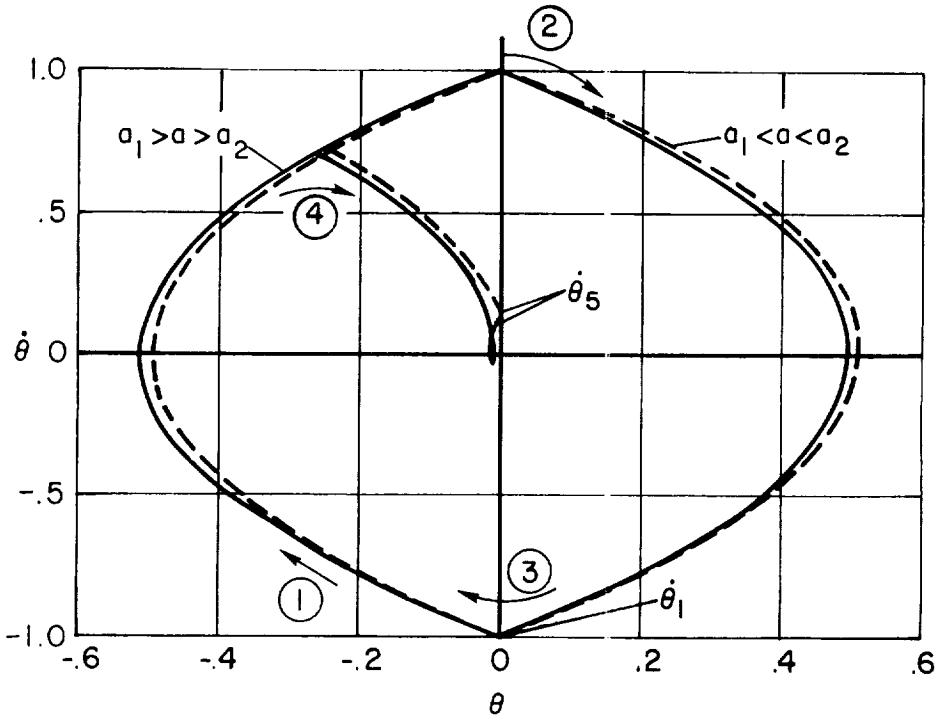

(a) Normalized phase plane trajectory; torque error = ±2 percent.

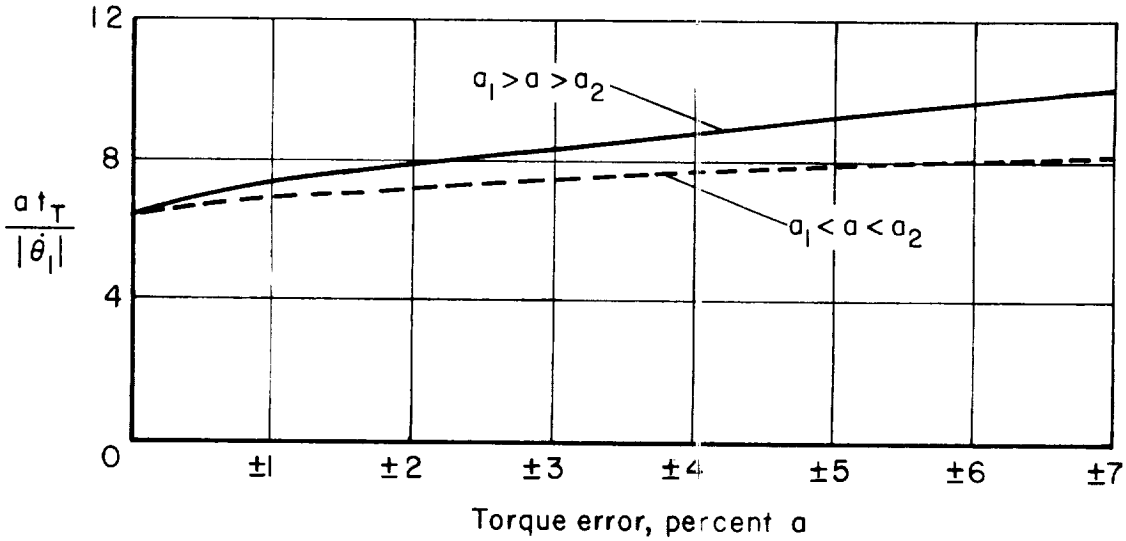

(b) Total settling time for an initial rate error.

Figure 6.- Effect of torque error on modified timer system.

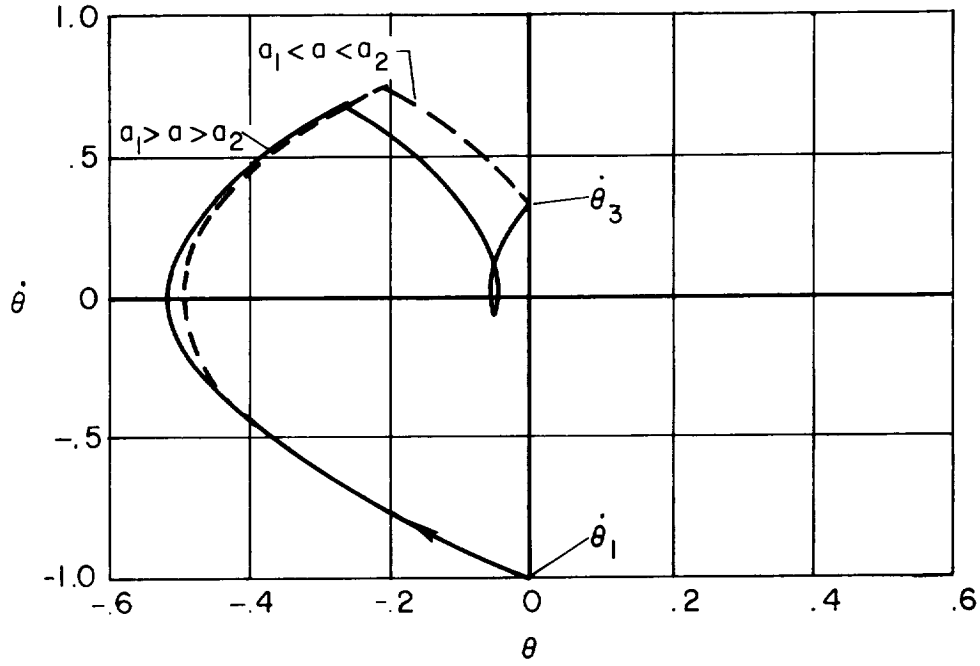

(a) Normalized phase plane trajectory; torque error = ±2 percent.

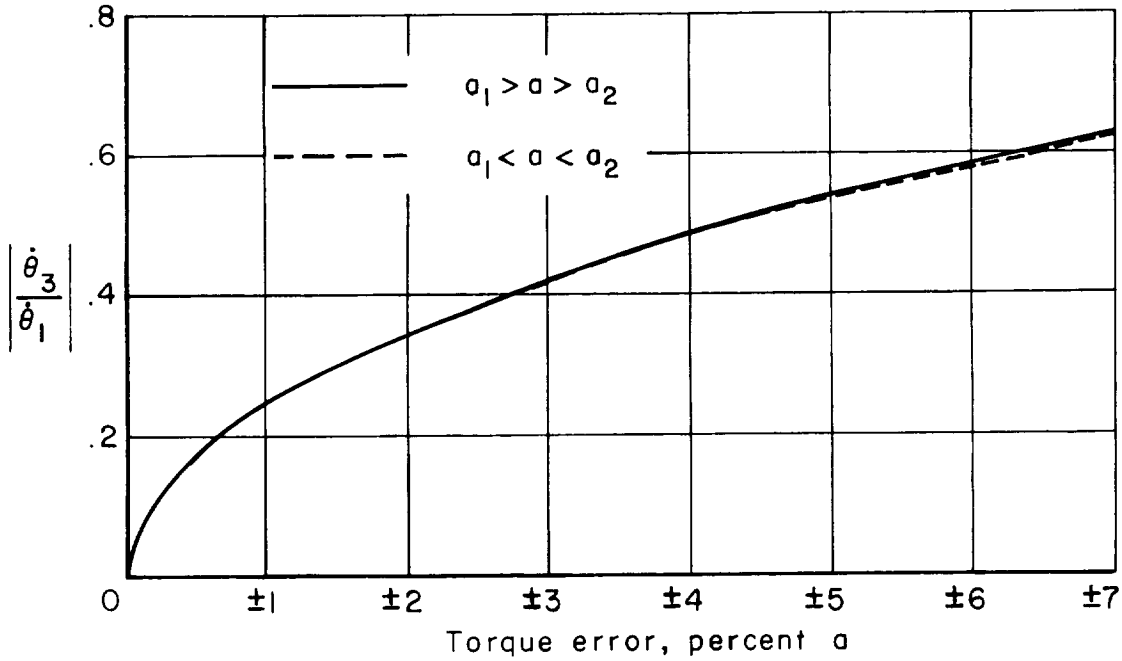

(b) Velocity decrement, per cycle.

Figure 7.- Effect of torque error on rate system response.

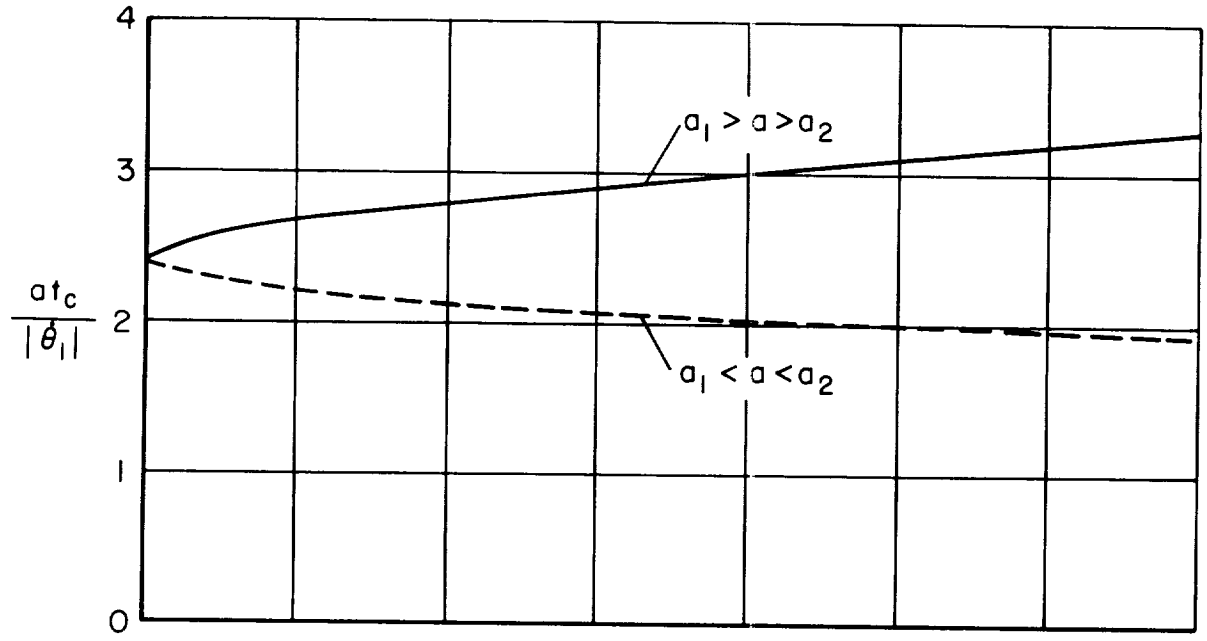

(c) Time, per cycle.

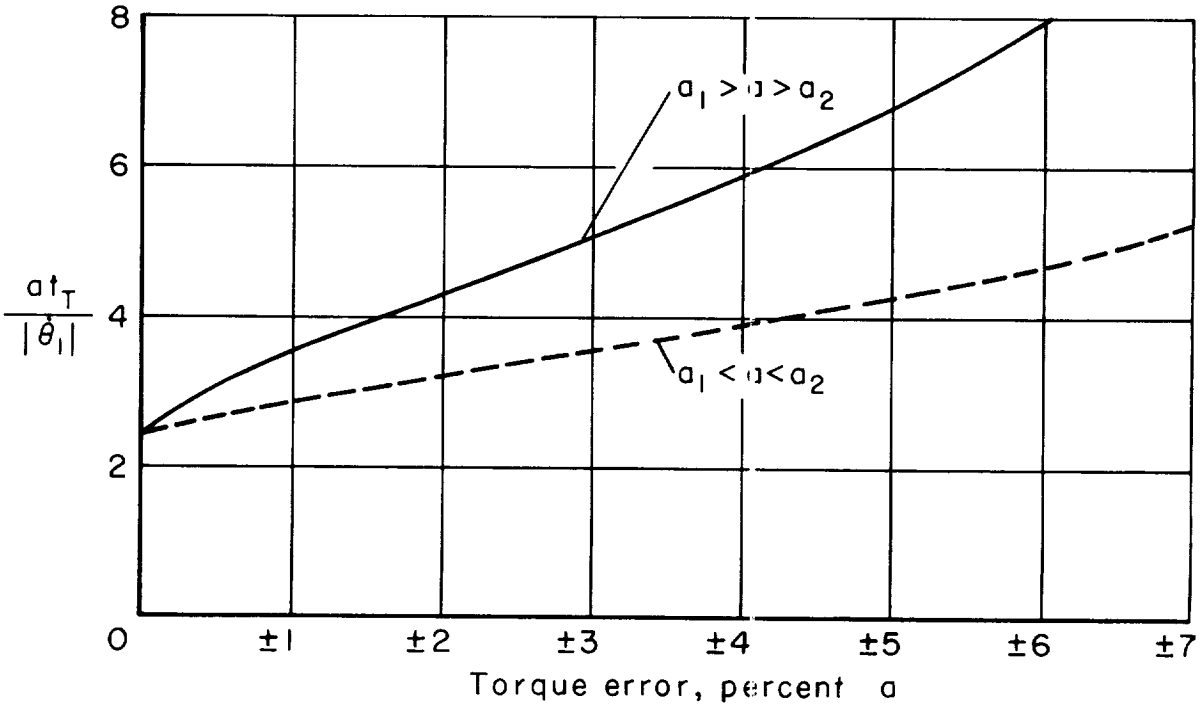

(d) Total settling time for an initial rate error.

Figure 7.- Concluded.

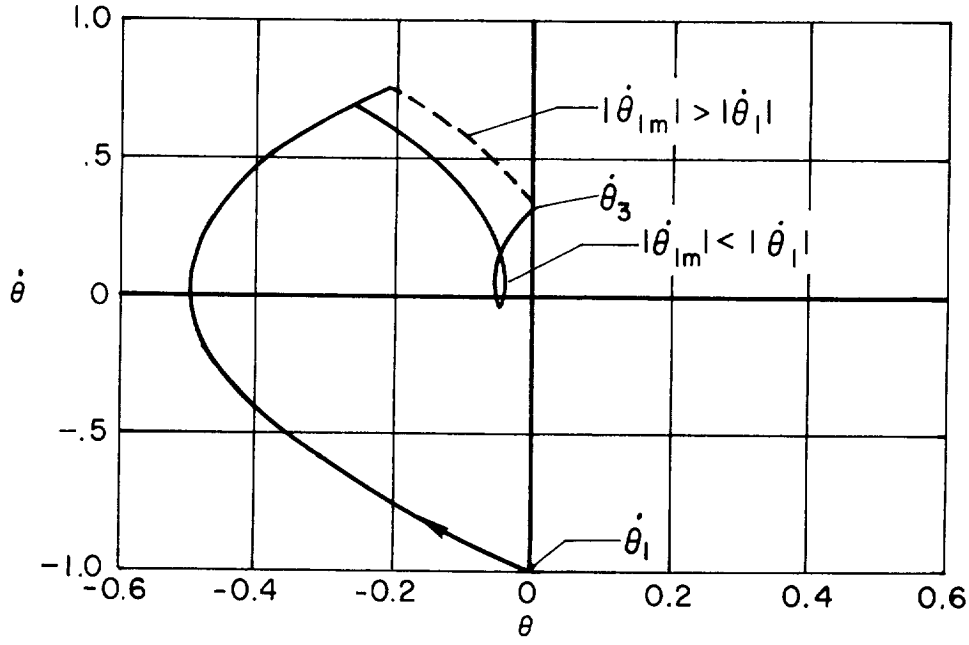

(a) Normalized phase plane trajectory; rate error = ±2 percent.

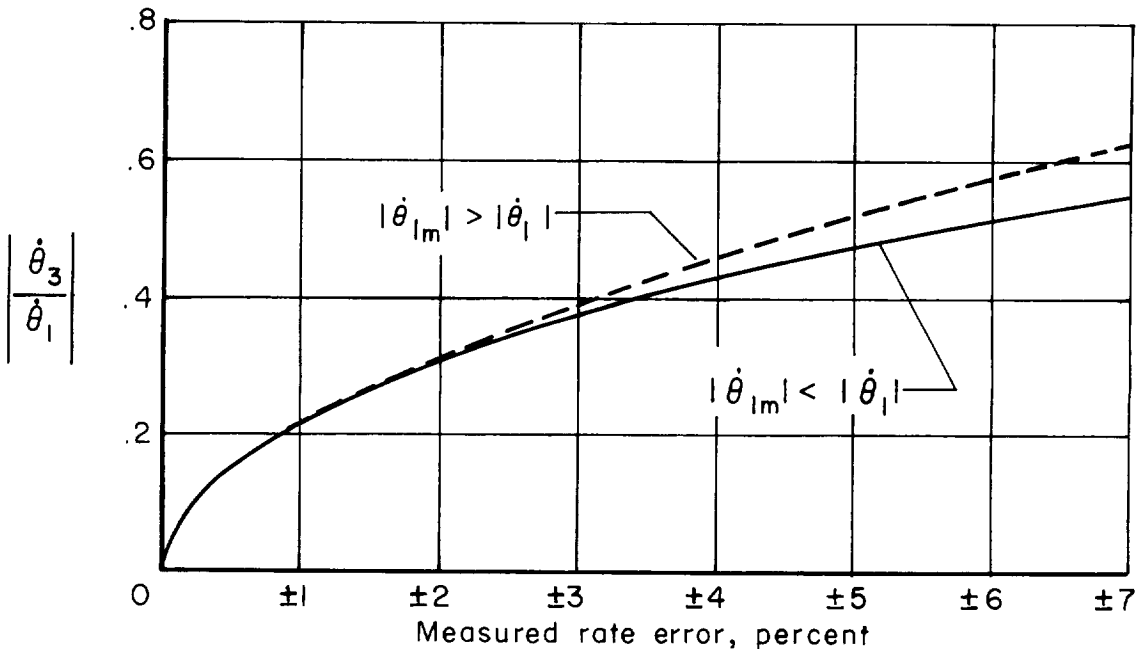

(b) Velocity decrement, per cycle.

Figure 8.- Effect of rate measurement error on rate system response.

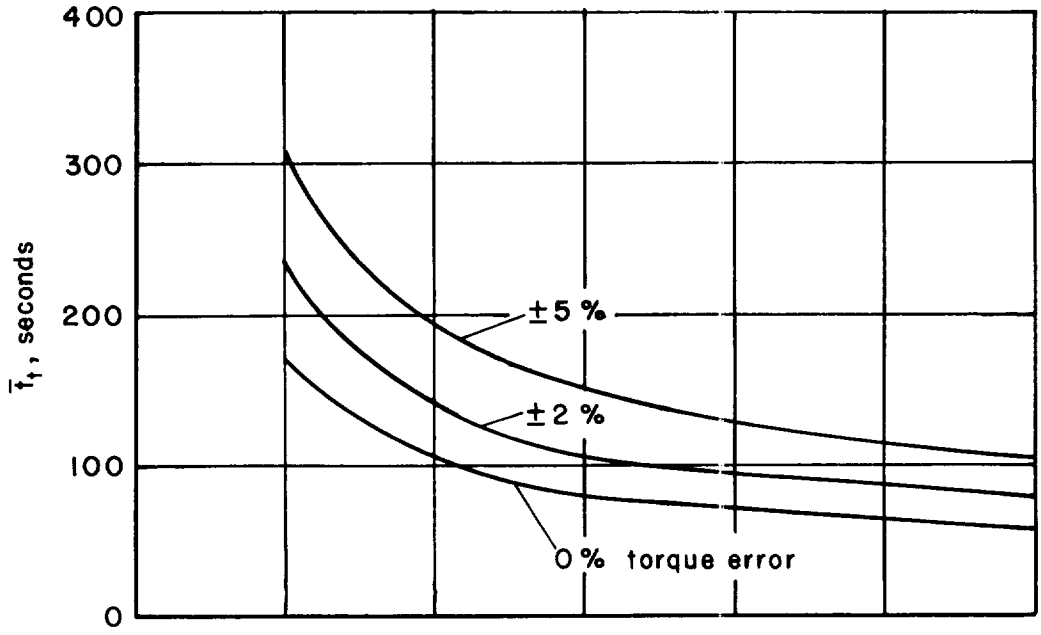

(c) Settling time.

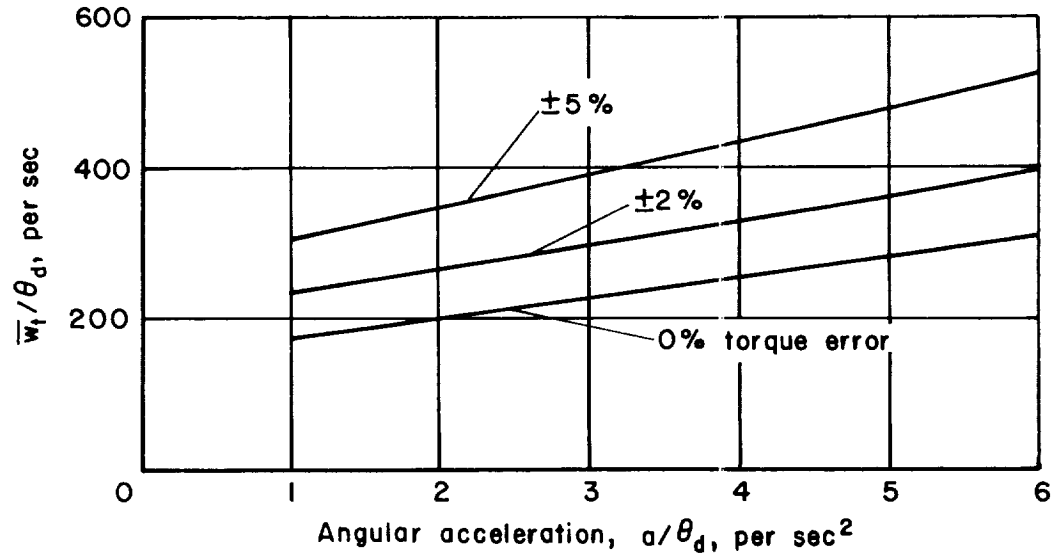

(d) Relative fuel consumption.

Figure 9.- Concluded.

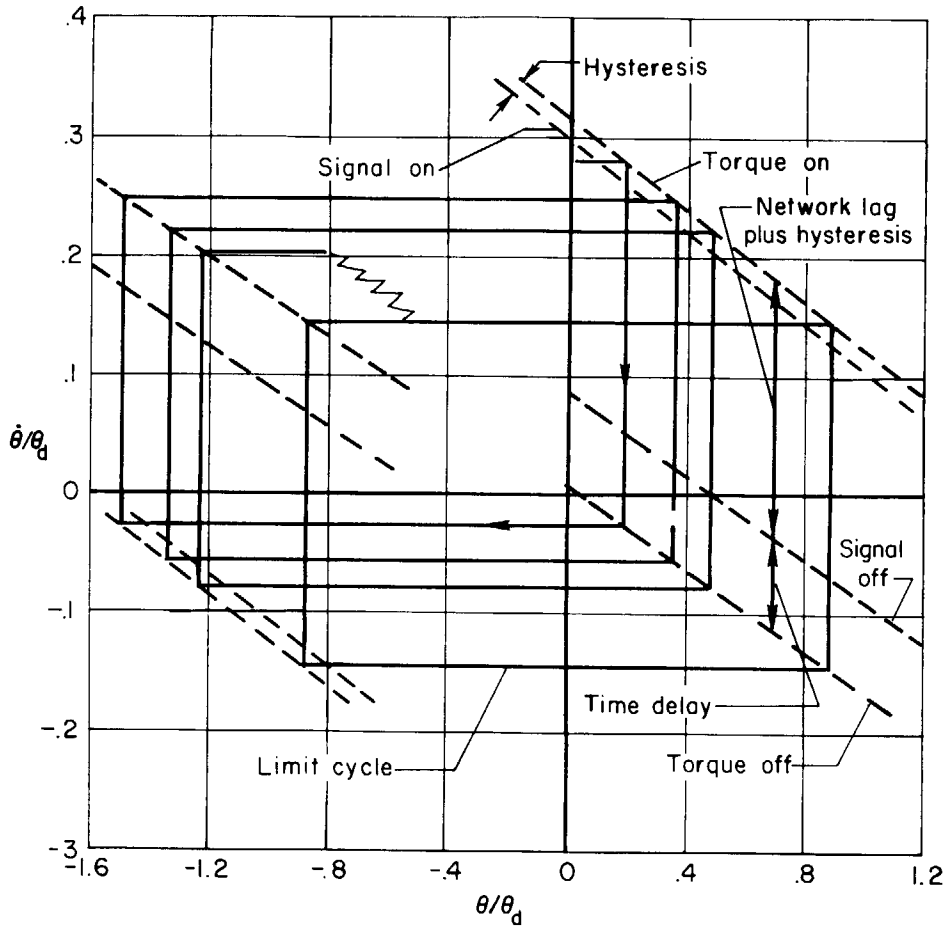

(a) No external disturbance.

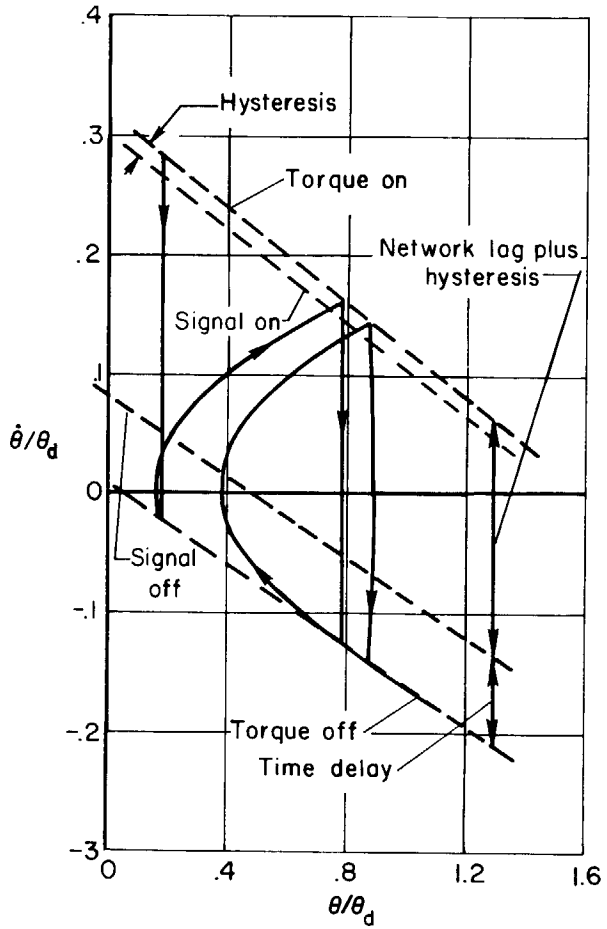

(b) External disturbance; $a_e/\theta_d = 0.02$ per sec^2.

Figure 10.- Effect of external torque on limit-cycle characteristics; $a/\theta_d = 2.5$ per sec^2, $h = 0.08\ \theta_d$, $t_d = 0.032$ sec, $K\dot{\theta} = 5$, $T = 0.5$.

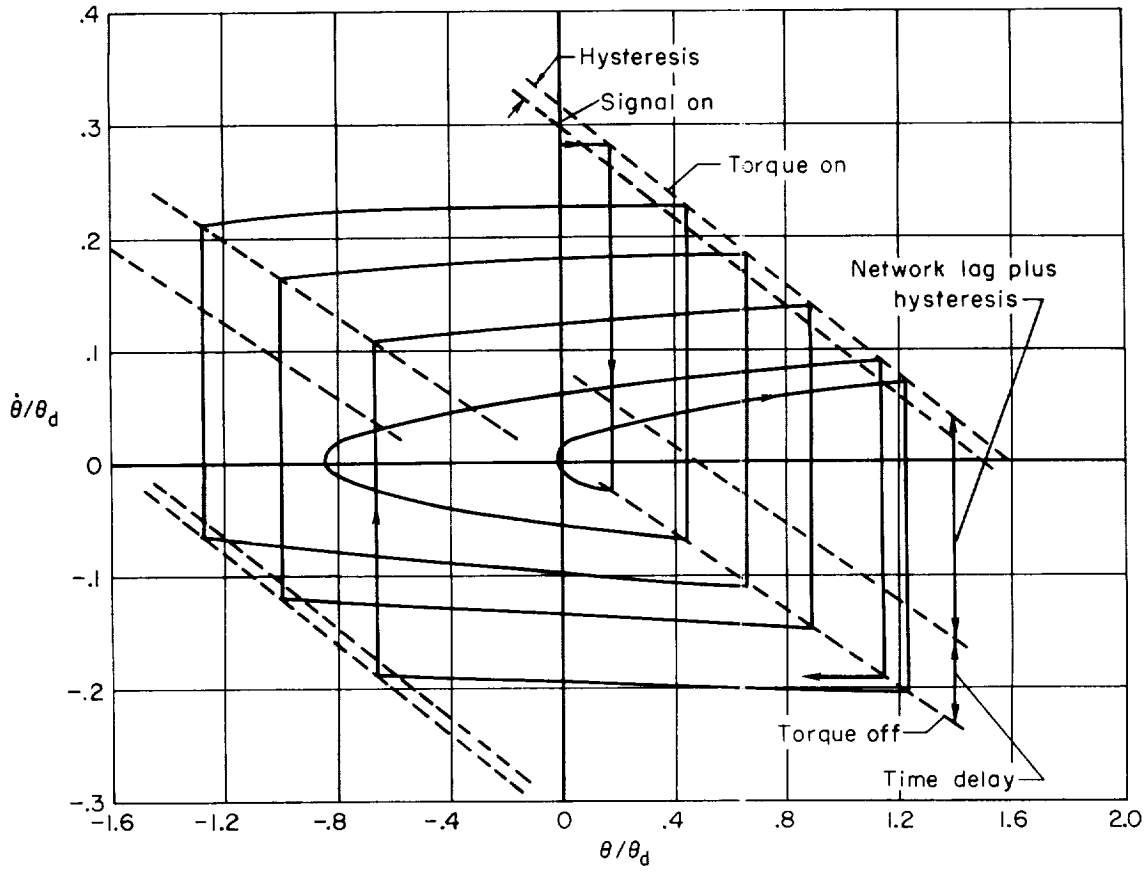

(c) External disturbance; a_e/θ_d = 0.002 per sec^2

Figure 10.- Concluded.

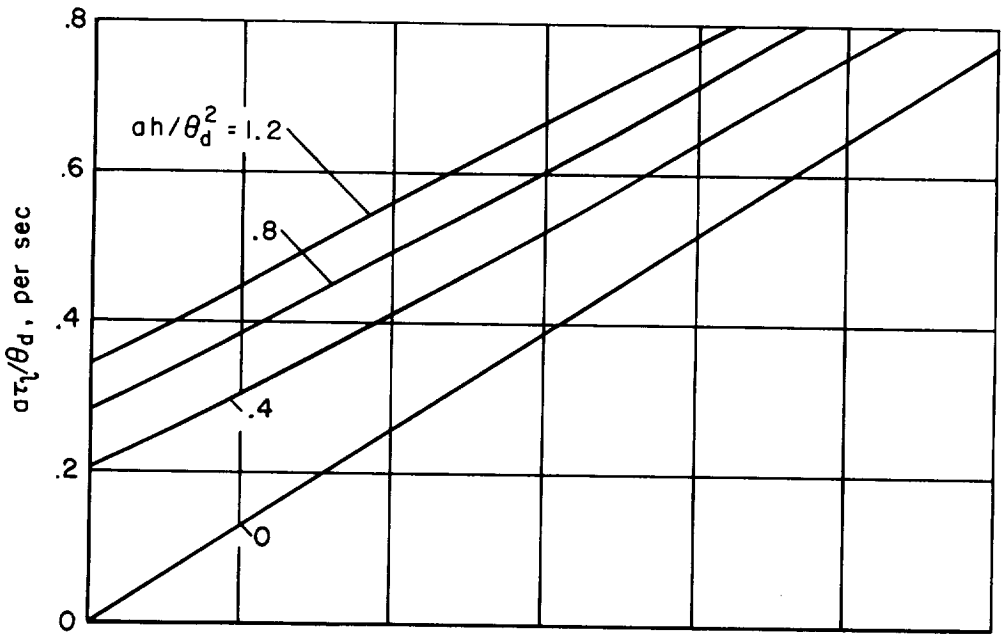

(a) $K_{\dot{\theta}}/T = 20$

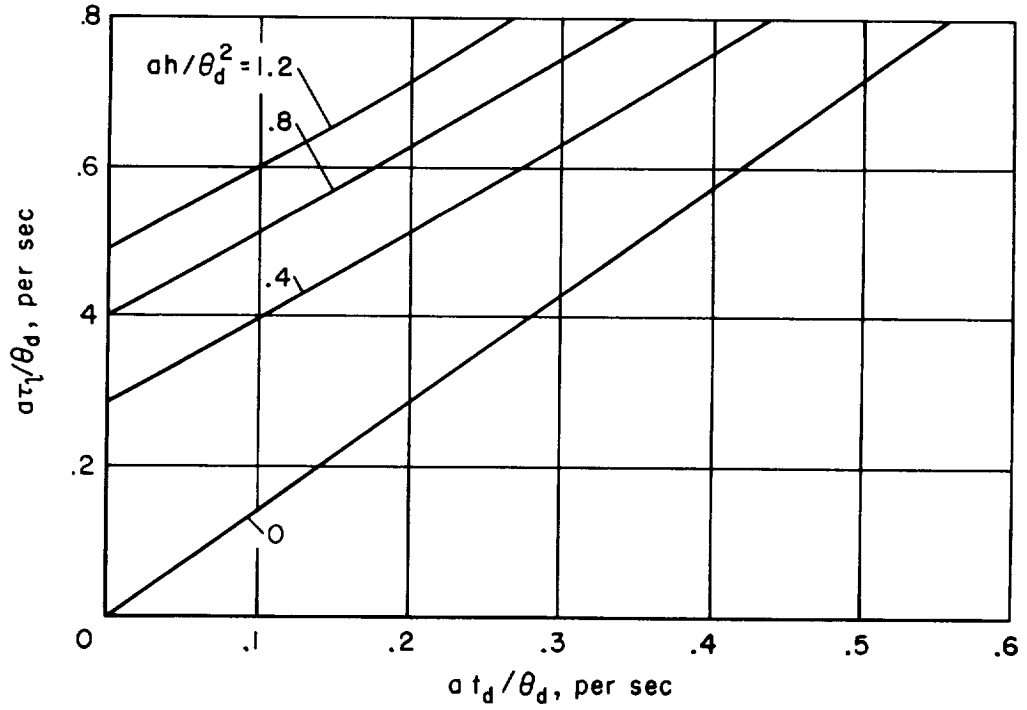

(b) $K_{\dot{\theta}}/T = 10$

Figure 11.- Effect of hysteresis, time delay, and lead network parameters on limit-cycle torque-on time.

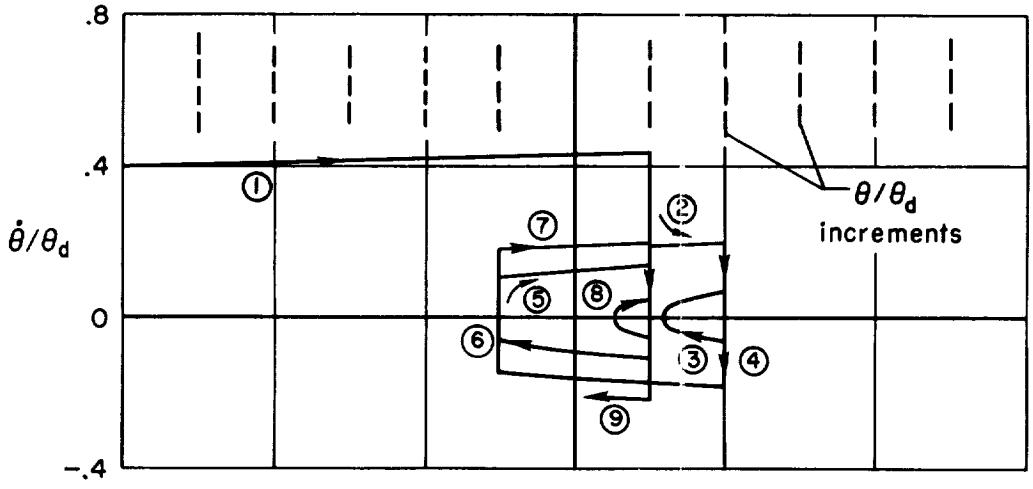

(a) External disturbance; a_e/θ_d = 0.002 per sec^2.

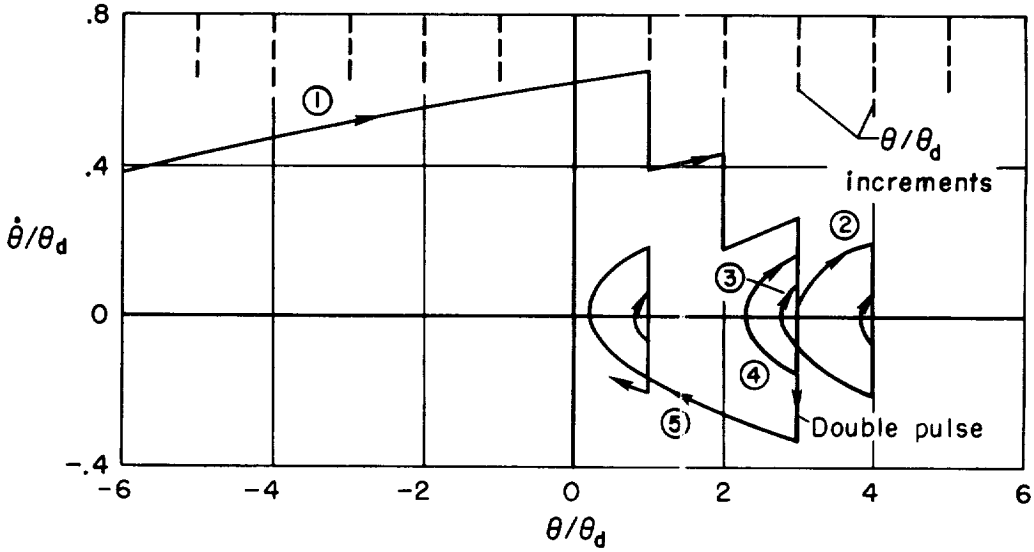

(b) External disturbance; a_e/θ_d = 0.02 per sec^2.

Figure 12.- Typical response for system with fixed pulses actuated by increments of attitude angle.